

**Physical Characterisation of the Test Lanes
in the
ITEP Dual Sensor Test
Oberjettenberg/Germany 2009**

H. Preetz, K. Takahashi, J. Igel



Hannover, February 2010

Content	Page
1 Introduction	1
1.1 Test site	1
1.2 Characterisation of soil.....	2
2 Methods.....	3
2.1 Methods of field measurements	3
2.2 Methods of laboratory measurements	4
3 General soil properties	6
3.1 Soil texture and humus content	6
4 Soil electric and dielectric properties and soil moisture contents	8
4.1 Field measurements.....	8
4.1.1 Daily time domain reflectometry (TDR) measurements in the test lanes	8
4.1.2 Soil moisture and temperature monitoring.....	9
4.1.3 Spatial variability of soil moisture and dielectric constant (relative permittivity).....	13
4.1.4 Ground-penetrating radar (GPR) measurements.....	16
4.1.5 Geoelectrical measurements.....	17
4.2 Laboratory measurements	28
4.2.1 Frequency dependence of electric conductivity.....	28
4.2.2 Frequency dependent dielectric constant (relative permittivity) of test targets.....	29
5 Soil magnetic properties.....	32
5.1 Field measurements.....	32
5.2 Laboratory measurements	35
5.2.1 Frequency dependence of magnetic susceptibility.....	35
6 Comprehensive classification of the test lanes.....	38

List of Figures	Page
Fig. 1: Site plan of the test and training lanes.	2
Fig. 2: Test lane 1.1 “Laterite“ with geoelectrical measuring array, viewing direction North (left hand). Training lane 1.3 “Laterite” in the front and lane 2.3 “Magnetite/Sand” in the picture center, viewing direction East (right hand).	3
Fig. 3: Texture triangle of the test soils.	6
Fig. 4: Cumulative grain size curves, showing the textures of the test soils.	6
Fig. 5: Mean values of volumetric soil moisture of 10 TDR daily measurements in the test lanes.	8
Fig. 6: TDR probes in test lane 1.1 “Laterite” before being buried and view of the soil surface.	10
Fig. 7: Soil moisture and temperature recording in Lane 1.1 - Laterite (soil moisture is given in $m^3/m^3 = \text{soil moisture}[\%]/100$).	10
Fig. 8: Soil moisture and temperature recording in Lane 1.2 - Laterite (soil moisture is given in $m^3/m^3 = \text{soil moisture}[\%]/100$).	11
Fig. 9: Soil moisture and temperature recording in Lane 2.1 - Magnetite/sand (soil moisture is given in $m^3/m^3 = \text{soil moisture}[\%]/100$).	11
Fig. 10: Soil moisture and temperature recording in Lane 2.2 - Magnetite/sand (soil moisture is given in $m^3/m^3 = \text{soil moisture}[\%]/100$).	12
Fig. 11: Soil moisture and temperature recording in Lane 3.1 – Humus (soil moisture is given in $m^3/m^3 = \text{soil moisture}[\%]/100$).	12
Fig. 12: Soil moisture and temperature recording in Lane 3.2 – Humus (soil moisture is given in $m^3/m^3 = \text{soil moisture}[\%]/100$).	13
Fig. 13: Soil moisture and dielectric constant in lane 1.3 Laterite, measured on 17.09.2009.	14
Fig. 14: Soil moisture and dielectric constant in lane 2.3 Magnetite/Sand, measured on 16.09.2009.	14
Fig. 15: Soil moisture and dielectric constant in lane 3.3 Humus, measured on 17.09.2009.	15
Fig. 16: GPR profiles along training lanes (1.5 GHz GSSI antenna). Top: Lane 2.4 (“Magnetite/Sand”), middle: Lane 1.4 (“Laterite”, clay loam), bottom: Lane 3.4 (“Humus”, loam, stony). PPM-2 mines were placed with a spacing of approximately 60 cm at a depths of 25, 20, 15, 10 and 5 cm (from left to right). The amplitudes are normalised to the maximum within each radargram.	16
Fig. 17: Geoelectrical measuring array in test lane 1.1 “Laterite”	17
Fig. 18: Soil electric conductivity at depths from 5 cm to 35 cm in Lane 1.1 (Laterite), measured on 21.09.2009.	18
Fig. 19: Probability density function (pdf) of the electric conductivity in Lane 1.1 (Laterite), measured on 21.09.2009.	18
Fig. 20: Soil electric conductivity at depths from 5 cm to 35 cm in Lane 2.2. (Magnetite) , measured on 23.09.2009.	19

List of Figures, continued**Page**

Fig. 21: Probability density function (pdf) of the electric conductivity in Lane 2.2 (Magnetite), measured on 23.09.2009.....	19
Fig. 22: Soil electric conductivity at depths from 5 cm to 35 cm in Lane 3.1 (Humus), measured on 22.09.2009.....	20
Fig. 23: Probability density function (pdf) of the electric conductivity in Lane 3.1 (Humus), measured on 22.09.2009.....	20
Fig. 24: Soil electric conductivity at depths from 5 cm to 35 cm in Lane 3.2 (Humus), measured on 22.09.2009.....	21
Fig. 25: Probability density function (pdf) of the electric conductivity in Lane 3.2 (Humus), measured on 22.09.2009.....	21
Fig. 26: Geoelectrical measuring array in training lanes 2.3 “Magnetite/Sand” (left hand) and 3.3 “Humus” (right hand).....	22
Fig. 27: Soil electric conductivity in Lane 1.3 (Laterite), measured on 17.09.2009.....	24
Fig. 28: Geostatistical analysis of topsoil electric conductivity ($z = 0.05- 0.20$ m) of Fig. 27. Boxplots (right), probability density function (top), semivariogram (bottom) which determines the correlation length of 30 cm.....	24
Fig. 29: Soil electric conductivity in Lane 2.3 (Magnetite), measured on 15.09.2009.....	25
Fig. 30: Geostatistical analysis of topsoil electric conductivity ($z = 0.05-0.20$ m) of Fig. 29. Boxplots (right), probability density function (top), semivariogram (bottom) which determines the correlation length of 50 cm.....	25
Fig. 31: Soil electric conductivity in Lane 3.3 (Humus), measured on 16.09.2009.....	26
Fig. 32: Geostatistical analysis of topsoil electric conductivity ($z = 0.05-0.20$ m) of Fig. 31. Boxplots (right), probability density function (top), semivariogram (bottom) which determines the correlation length of 25 cm.....	26
Fig. 33: Laboratory measurements of soil electric conductivity by spectral induced polarization (SIP). The frequency dependence over one decade is given in parentheses.	28
Fig. 34: Real part of the frequency dependent dielectric constant of the ERA calibration target casing (left) and the wax filling (right).	29
Fig. 35: Real part of the frequency dependent dielectric constant of the PPM-2 plastic body(left) and the silicone filling “3110 Base + Catalyst 1” (right).....	30
Fig. 36: Real part (left) and imaginary part (right) of the frequency dependent dielectric constant of the Gyata-64 (PMN) plastic casing.	30
Fig. 37: Real part (left) and imaginary part (right) of the frequency dependent dielectric constant of the Gyata-64 (PMN) rubber cap.	31
Fig. 38: Soil magnetic susceptibility in Lane 1.3 (Laterite), measured with field loop.....	33
Fig. 39: Soil magnetic susceptibility in Lane 2.3 (Magnetite), measured with field loop.	33

List of Figures, continued	Page
Fig. 40: Soil magnetic susceptibility in Lane 3.3 (Humus), measured with field loop.....	34
Fig. 41: Frequency dependent magnetic susceptibility in Lane 1.3 (Laterite). The frequency dependence is given for one decade (100 Hz vs. 1000 Hz).	35
Fig. 42: Frequency dependent magnetic susceptibility in Lane 2.3 (Magnetite). The frequency dependence is given for one decade (100 Hz vs. 1000 Hz).	36
Fig. 43: Frequency dependent magnetic susceptibility in Lane 3.1 (Humus). The frequency dependence is given for one decade (100 Hz vs. 1000 Hz).	36
Fig. 44: Frequency dependent magnetic susceptibility in Lane 3.3 (Humus).....	37

List of Tables

Table 1: Test lanes and training lanes and conducted soil investigations. Numbers in parentheses indicate sections describing the results.....	4
Table 2: Soil texture and humus contents of test soils.	7
Table 3: Mean values of 10 TDR measurements in the particular test lanes.	9
Table 4: Mean values of 10 soil temperature measurements in the particular test lanes.	9
Table 5: Parameters describing the spatial variability of soil moisture.	15
Table 6: Summary of soil electric parameters of the test lanes. The standard deviation is also given as a measure of variability in %, although conductivity distribution is similar to a log-normal distribution. One has to notice that standard deviation does not describe the 68% population in this case.....	27
Table 7: Summary of soil magnetic field parameters of the test lanes.	34
Table 8: Summary of soil magnetic laboratory parameters of the test lanes.	37
Table 9: Indicative values of magnetic susceptibility that can be expected for soil effects for single frequency continuous wave metal detectors (CEN 2008).	38
Table 10: Indicative values classifying the influence of frequency dependent susceptibility on multi-frequency continuous wave and pulse induction detectors (CEN, 2008).....	38
Table 11: Estimated impact of soil on the performance of detection techniques.	38

1 Introduction

The landmine detection test facility in the Bundeswehr Technical Center for Protective and Special Technologies in Oberjettenberg, Germany (WTD 52), which belongs to the Federal Office of Defense Technology and Procurement, was used to carry out the metal detector and dual sensor trial of ITEP 2009 (International Test and Evaluation Program for Humanitarian Demining).

To document the test conditions a pedological and geophysical investigation of the test lane soils was carried out. The aim of the investigation was to describe the similarities and differences of the test lanes and to quantify soil parameters that have an effect on the performance of the detection techniques used. Since the techniques used in this trial comprise metal detectors, based on electromagnetic induction (EMI), and ground-penetrating radar (GPR) as well, a wide range of soil physical parameters has to be considered. Metal detectors are mainly influenced by soil magnetic properties whereas GPR sensors are subject to soil electric and dielectric properties. In order to complete the investigation the dielectric properties of some test targets were also analysed by laboratory measurements.

1.1 Test site

Soil material with different origin and different physical properties was used to build the test lanes to ensure that a range of various soil influences was covered by the test arrangement to provide realistic as well as challenging test conditions.

Six test lanes and six training lanes were built in the facility to conduct the test and the site plan of these lanes is depicted in Fig. 1 (cf. Fig. 2). The test lanes have a width of 1.3 or 1.5 m, a depth of 0.6 m and a length of 20 or 30 m. The lanes are surrounded by the local natural soil and they are bordered by either wooden boards or metal-free concrete. There is no sealing at the bottom of the lanes, but a gravel layer to ensure a proper drainage of percolating water.

The test lanes were specially prepared for the dual sensor test and test targets were buried before the geophysical investigations were carried out. Because of their interfering influence on geophysical soil investigation most of the measurements were carried out on the corresponding training lanes instead, assuming that they have similar properties. In Table 1 the test lanes are listed including the investigations that were carried out there in detail.

1.2 Characterisation of soil

The following list gives a brief description of the different soil materials in the test lanes:

- Lanes 1.1, 1.2, 1.3 and 1.4 - “Laterite”
This soil material is a tropical soil formation from the Tertiary period. It stems from a former bauxite pit, located in the median range mountain of the Vogelsberg area in the middle of Germany. Its parent rock is basalt. The texture is Clay loam with a small stone content (basalt) of approximately 2-5 %. Laterites are the most frequent tropical soil formation and the Laterite in the test lane provides the same physical and chemical features like those in the recent tropics.
- Lanes 2.1, 2.2, 2.3 and 2.4 - “Magnetite/Sand”
The soil material in these lanes is a synthetic mixture of calcareous sand with industrially manufactured magnetite. The texture is coarse Sand with a low content of fine gravel (2-5 %).
- Lane 3.1 - “Humus”
The parent material of this top soil material is loess and the texture is loam with a low content of fine gravel. Its regional provenance is in the region of the foothills of the Bavarian Alps. Its humus content is 2.7 %.
- Lanes 3.2, 3.3 and 3.4 - “Humus”
This topsoil material stems from a forest in the Bavarian Alps region and its texture is loam. Its main features are the high humus content and the high stone content which is about 30-40 %.

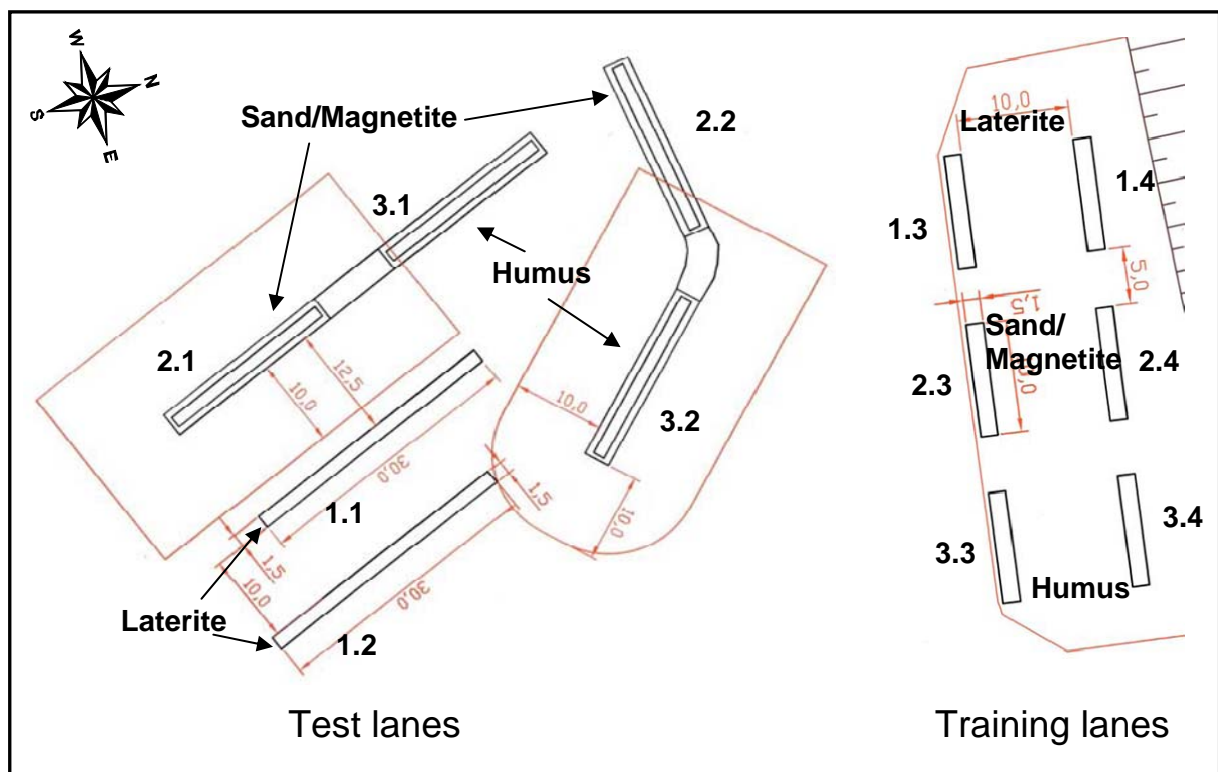


Fig. 1: Site plan of the test and training lanes.



Fig. 2: Test lane 1.1 “Laterite“ with geoelectrical measuring array, viewing direction North (left hand). Training lane 1.3 “Laterite” in the front and lane 2.3 “Magnetite/Sand” in the picture center, viewing direction East (right hand).

2 Methods

The following instruments and methods were used to analyse the individual soil properties. An overview on the parameters measured in the individual test and training lanes is given in Table 1.

2.1 Methods of field measurements

- Magnetic susceptibility measurements
Bartington MS2 magnetic susceptibility meter and MS2D field loop (18 cm diameter).
- Soil moisture and dielectric constant
Time domain reflectometry (TDR) probe FOM/mts (Institute of Agrophysics of the Polish Academy of Sciences)
- Soil moisture and temperature monitoring
Soil moisture and temperature sensor EC-TM (Decagon Device, Inc.) These sensors were provided for the test by Dr. Todd R. Higgins from the Land Mine Detection Research Center, Lincoln University, Jefferson City, MO, USA. The installation of the sensors in the test lanes was completed by LIAG and the subsequent readout of the stored data was done by the staff of the Technical Center.
- Electric Conductivity
GeoServe Resecs multi-channel device, measurement in different dipole-dipole configurations with 10 cm electrode spacing along profiles or inside array.
- GPR measurements
Geophysical Survey Systems International (GSSI) SIR-3000 and 1.5 GHz shielded antennas.

2.2 Methods of laboratory measurements

- Soil texture
Separation of the fraction > 63 µm after dispersion by wet sieving. Further analyse of the fraction > 63 µm by dry sieving. Analysis of the fraction < 63 µm after dispersion by means of the Sedigraph 5100 (Micromeritics GmbH).
- Soil humus content
Analysis of organic and total carbon content after dry combustion according to DIN ISO 10694.
- Magnetic susceptibility
Bartington MS2B dual frequency sensor, Magnon VFSM susceptibility bridge.
- Electric conductivity, frequency dependence
SIP Fuchs laboratory device.
- Dielectric constant, frequency dependence
The investigation of the test targets was carried out in the Geophysical Institute of the University Frankfurt/Main by means of a plate-type capacitor in the frequency range 1 MHz – 3 GHz. The measuring instrument consists of an impedance analyser (Agilent) and a measuring cell (Novocontrol).

Table 1: Test lanes and training lanes and conducted soil investigations. Numbers in parentheses indicate sections describing the results.

test lane	field measurements					
	magnetic susceptibility (5.1)	soil moisture (4.1.1, 4.1.2, 4.1.3)	dielectric constant/permittivity (4.1.1., 4.1.3)	Soil temperature (4.1.2)	electric conductivity (4.1.5)	GPR measurements (4.1.4)
Laterite 1.1		X	X	X	X	
1.2		X	X	X		
1.3	X				X	
1.4						X
Magnetite 2.1		X	X	X		
2.2		X	X	X	X	
2.3	X				X	
2.4						X
Humus 3.1		X	X	X	X	
Humus 3.2		X	X	X	X	
3.3	X				X	
3.4						X

Table 1: continued.

test lane	laboratory measurements					
	soil texture (3.1)	humus content (3.1)	magnetic susceptibility absolute (5.2)	magnetic susceptibility frequency dependent (5.2)	frequency dependent electric conductivity (4.2.1)	dielectric constant/ permittivity frequency dependent (4.2.2)
Laterite 1.1						
1.2						
1.3	X	X	X	X	X	
1.4						
Magnetite 2.1						
2.2						
2.3	X	X	X	X	X	
2.4						
Humus 3.1	X	X	X	X	X	
Humus 3.2	X	X				
3.3			X	X	X	
3.4						
test targets						X

3 General soil properties

3.1 Soil texture and humus content

The grain size distributions of the test lanes are different as shown in Figs. 3, 4 and Table 2. From these analyses the grain size of each test soil can be classified as follows:

- Lanes 1.1, 1.2, 1.3 and 1.4, “Laterite” - Clay Loam
- Lanes 2.1, 2.2, 2.3 and 2.4, “Magnetite/Sand” - Sand
- Lane 3.1, “Humus” - Loam
- Lanes 3.2, 3.3 and 3.4, “Humus” - Loam

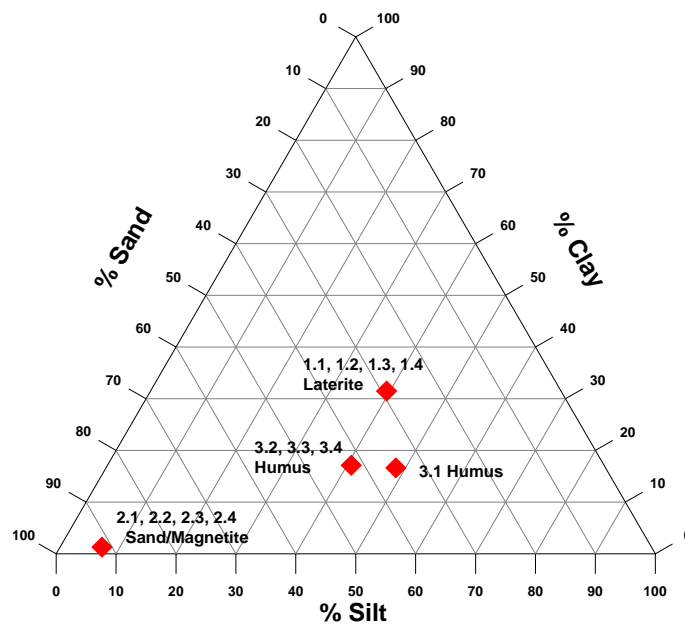


Fig. 3: Texture triangle of the test soils.

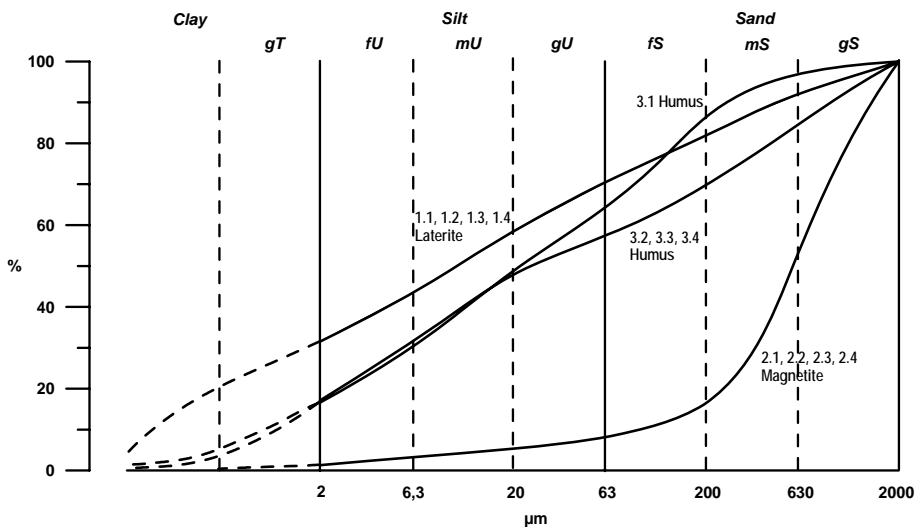


Fig. 4: Cumulative grain size curves, showing the textures of the test soils.

Table 2: Soil texture and humus contents of test soils.

		1.3 Laterite	2.3 Magnetite	3.1 Humus	3.3 Humus
clay	% of mineral soil	31.5	1.3	16.6	17.1
silt		39.4	7.0	48.4	40.7
sand		29.1	91.7	35.0	42.2
humus	% of total soil	0.8	< 0.5	2.7	12.4

Since many physical soil features such as pore size distribution and related soil water content are strongly correlated to the grain size distribution, the different textures of the test lanes represent a wide variety of possible effects on GPR performance. In general the loam and clay loam textures have much more medium and fine pores than sand and thus a much higher capacity for water retention. Additionally, the clay contents of the “Laterite” (Lanes 1.1-1.4) and the “Humus” lanes (Lanes 3.1-3.4) and the high humus content of the latter (Lanes 3.2-3.4) may contribute to a higher electric conductivity of these soils. This is due to the very high internal surface area of these micro-sized particles and the related high cation exchange capacity yielding a high electric conductivity of the pore fluid. Besides, these materials possess a high surface conductivity. High electric conductivity means high damping of electromagnetic waves that can have an impact on GPR performance.

A further big influence on the performance of GPR is rising from the high stone content in the “Humus” lanes (Lanes 3.2-3.4). These stones will be detected as clutter. In particular if they have the same size as the landmines they cause similar radar signatures and thus increase the disruption of the detectability of targets. The lower stone content in the “Laterite” lanes (Lanes 1.1-1.4) may also lead to only some clutter effects in places.

The coarse sand of the “Sand/Magnetite” lane (Lanes 2.1-2.4), on the other hand, is expected to provide no negative impact on GPR performance at all. This is due to the low electric conductivity of the coarse particles and the high porosity of the material and the related low water content. Additionally this artificial substrate is very homogeneous which a benign feature is also for GPR.

4 Soil electric and dielectric properties and soil moisture contents

4.1 Field measurements

4.1.1 Daily time domain reflectometry (TDR) measurements in the test lanes

Measurements of volumetric soil water contents and temperatures in the test lanes were carried out daily during the entire period of the detector test by the staff of the Technical Center using a TDR probe. For this purpose 10 single measurements were collected on 10 equally spaced positions in each individual test lane. The moisture values measured by TDR correspond to the average of the upper 10 cm of the soil. For each test lane, the mean values of the 10 single moisture measurements are given in Fig. 5 and Table 3. Temperature data are given in Table 4. This investigation was done to monitor the test conditions, especially concerning GPR performance and their possible change during the test period.

Figure 5 demonstrates the difference in the general soil water content between the sand in the “Magnetite” test lane (Lanes 2.1 and 2.2) and the other substrates that are more loamy, clayey and humous than the “Magnetite”. Further, it depicts the significant rise of the water contents in the last two weeks of the trial which is due to the change of weather from warm and dry to cold rainy and finally snowy.

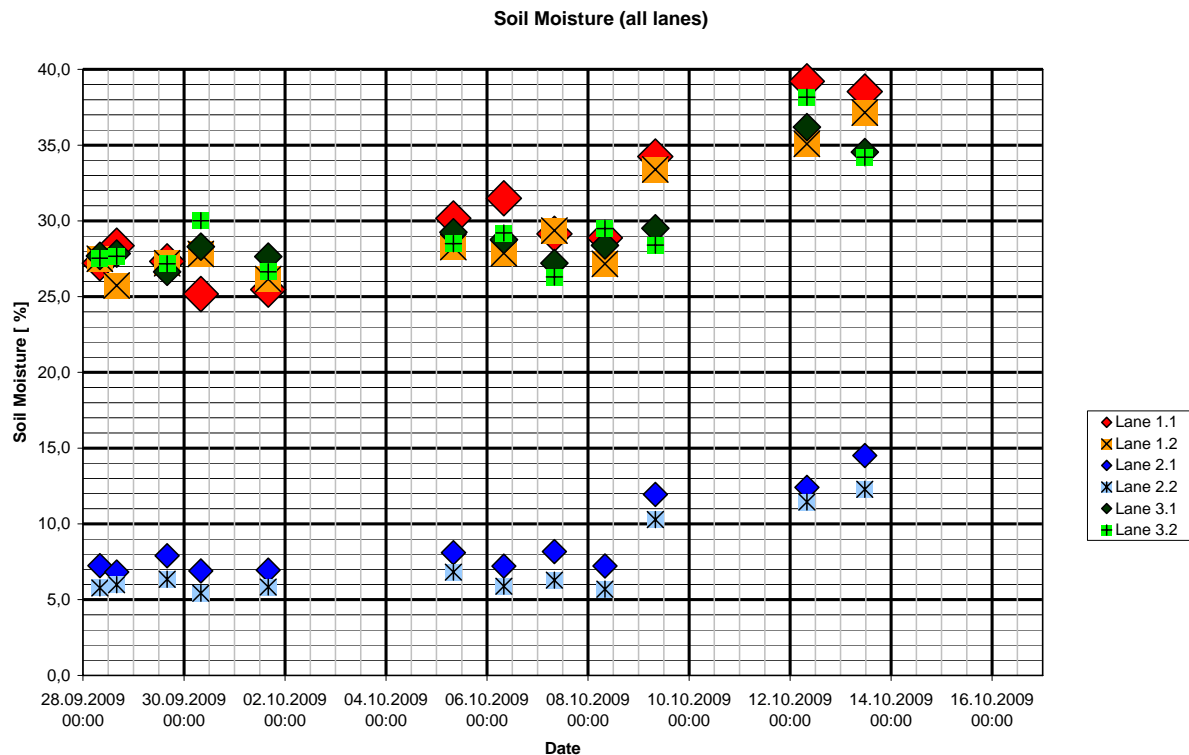


Fig. 5: Mean values of volumetric soil moisture of 10 TDR daily measurements in the test lanes.

Table 3: Mean values of 10 TDR measurements in the particular test lanes.

Date	Lane 1.1 Laterite		Lane 1.2 Laterite		Lane 2.1 Magnetite		Lane 2.2 Magnetite		Lane 3.1 Humus		Lane 3.2 Humus	
	soil moisture [vol%] / dielectric constant []											
	[%]	[]	[%]	[]	[%]	[]	[%]	[]	[%]	[]	[%]	[]
28.09.2009	28,4	17,36	27,5	16,72	7,3	4,73	6,0	4,20	27,7	16,63	27,5	16,59
29.09.2009	27,3	16,52	28,7	17,29	7,9	5,00	6,4	4,35	26,6	15,90	27,2	16,37
30.09.2009	25,2	15,15	27,8	16,88	6,9	4,61	5,4	4,01	28,3	17,08	30,0	18,67
01.10.2009	25,5	15,48	26,2	15,76	7,0	4,60	5,8	4,15	27,6	16,58	26,6	16,13
05.10.2009	30,2	18,99	28,3	17,40	8,1	5,10	6,8	4,53	29,3	17,86	28,5	17,38
06.10.2009	31,5	19,97	27,9	16,91	7,2	4,70	5,9	4,15	28,8	17,48	29,2	17,92
07.10.2009	29,1	18,03	29,4	18,14	8,2	5,12	6,3	4,33	27,2	16,21	26,3	15,72
08.10.2009	28,9	17,71	27,2	16,37	7,2	4,72	5,7	4,12	28,4	17,13	29,5	18,13
09.10.2009	34,2	22,05	33,4	21,37	11,9	6,90	10,3	6,05	29,5	17,84	28,4	17,25
12.10.2009	39,2	26,85	35,1	22,86	12,4	7,20	11,5	6,67	36,2	23,34	38,2	24,99
13.10.2009	38,5	25,49	37,2	24,38	14,5	8,27	12,3	7,10	34,5	21,67	34,2	22,14

Table 4: Mean values of 10 soil temperature measurements in the particular test lanes.

Date	Lane 1.1 Laterite		Lane 1.2 Laterite		Lane 2.1 Magnetite		Lane 2.2 Magnetite		Lane 3.1 Humus		Lane 3.2 Humus	
	soil temperature [°C]											
28.09.2009	21,9	23,3	22,8	21,4	20,1	19,4						
29.09.2009	21,8	21,1	22,0	23,2	21,9	21,9						
30.09.2009	13,6	13,7	14,5	16,7	20,1	19,6						
01.10.2009	19,7	20,2	20,9	20,4	23,7	20,4						
05.10.2009	10,0	13,0	9,7	9,3	13,1	10,4						
06.10.2009	12,6	13,1	12,7	14,0	12,1	12,3						
07.10.2009	14,0	14,3	15,1	15,4	15,2	14,3						
08.10.2009	12,9	12,9	13,2	13,7	17,2	13,6						
09.10.2009	16,7	16,2	16,3	16,5	17,7	17,0						
12.10.2009	10,6	7,9	7,4	7,7	8,2	7,8						
13.10.2009	9,5	5,9	5,1	4,9	5,3	5,2						

4.1.2 Soil moisture and temperature monitoring

Continuous measurements of soil moisture and temperature were carried out with permanently installed TDR probes at one position of each test lane. The probes were installed at depths of 2, 5, 10, 15 and 20 cm (see Fig. 6) and Figs. 7-12 depict the soil moisture values in depths of 2, 10 and 20 cm to assure the clarity of the graph. Additionally, the temperature measured at the depth of 2 cm is given. The measurements started on 18.09. or 21.09. and lasted for 28 or 25 days, respectively.

All of the graphs in Figs. 7-12 demonstrate that the conditions in the test lanes remained constant during the trial with exception of the last week. Then a sudden change of weather occurred and the mild and dry autumn weather became rainy and cold. On the last three days of the test there was even a snow layer on the test lanes.



Fig. 6: TDR probes in test lane 1.1 “Laterite” before being buried and view of the soil surface.

The temperature curves in the graphs result from a measurement at 2 cm depth and thus correlate strongly to the diurnal temperature variation in air or are influenced by direct warming of the soil by solar radiation. This holds especially for the temperature curve of the coarse sand of the “Magnetite/Sand” test lanes (Lanes 2.1 and 2.2). These substrates have a high volume of coarse pores that are filled with air and accordingly lower moisture content. Therefore, the variation of daily and nightly temperature is the biggest among other soils. The daily peak of the temperature amplitude is also registered until the depth of 10 cm by the probes measuring soil moisture. They are obviously temperature sensitive. The decrease of the air and soil temperature in the last week accompanied a significant rise of soil moisture in the “Magnetite” (Lanes 2.1 and 2.2) and “Humus”-test lanes (Lanes 3.1 and 3.2). The rise in the “Laterite”-test lanes (Lanes 1.1 and 1.2) is only moderate because they had already high water contents of approximately 35 % from the beginning which could not be highly enlarged because their pore volume seemed to be nearly filled up so that the additional rain water percolated or ran off the surface.

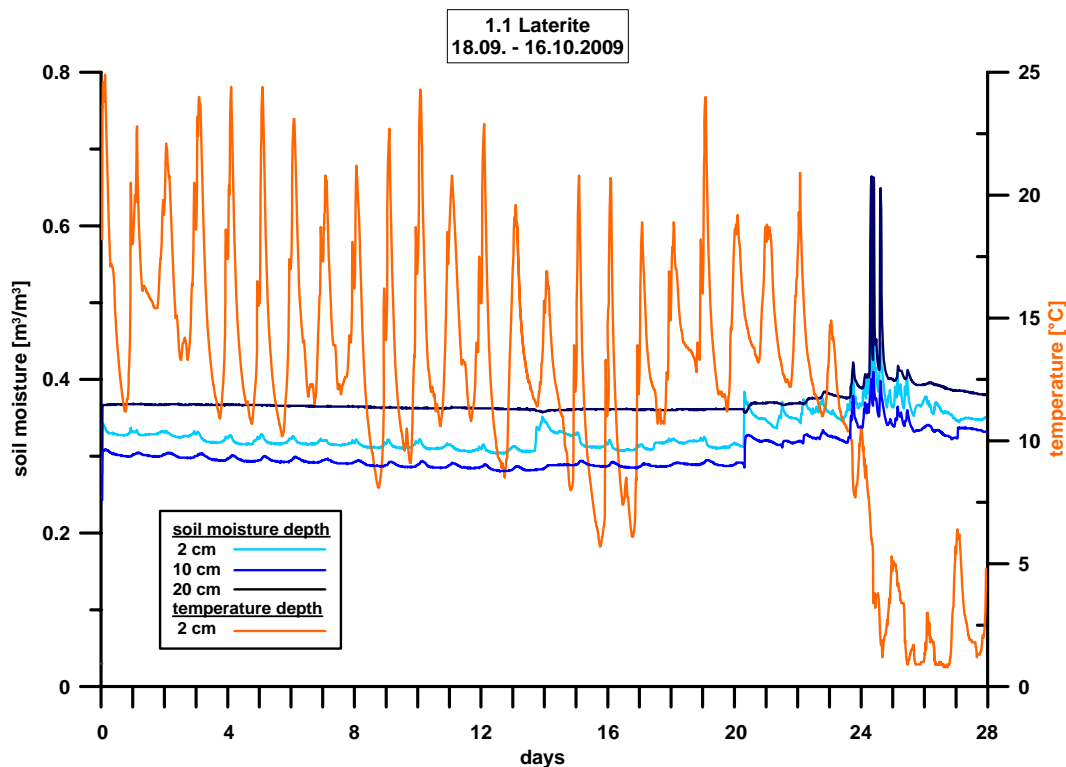


Fig. 7: Soil moisture and temperature recording in Lane 1.1 - Laterite (soil moisture is given in $\text{m}^3/\text{m}^3 = \text{soil moisture}[\%]/100$).

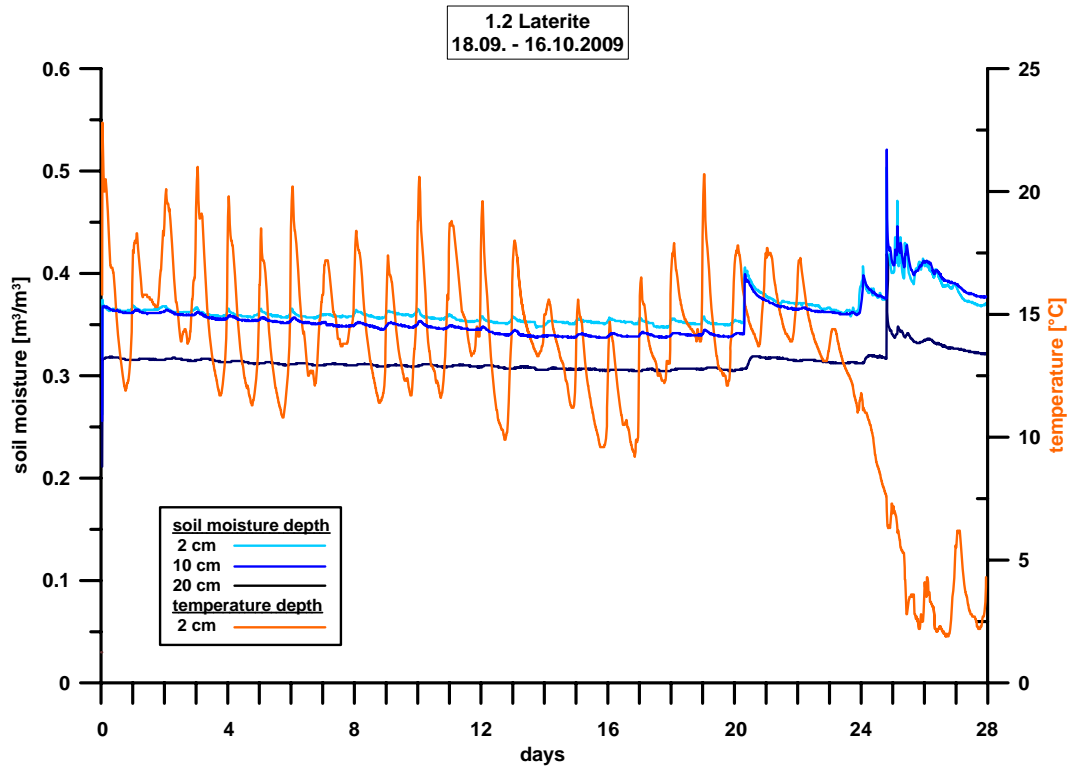


Fig. 8: Soil moisture and temperature recording in Lane 1.2 - Laterite (soil moisture is given in $\text{m}^3/\text{m}^3 = \text{soil moisture}[\%]/100$).

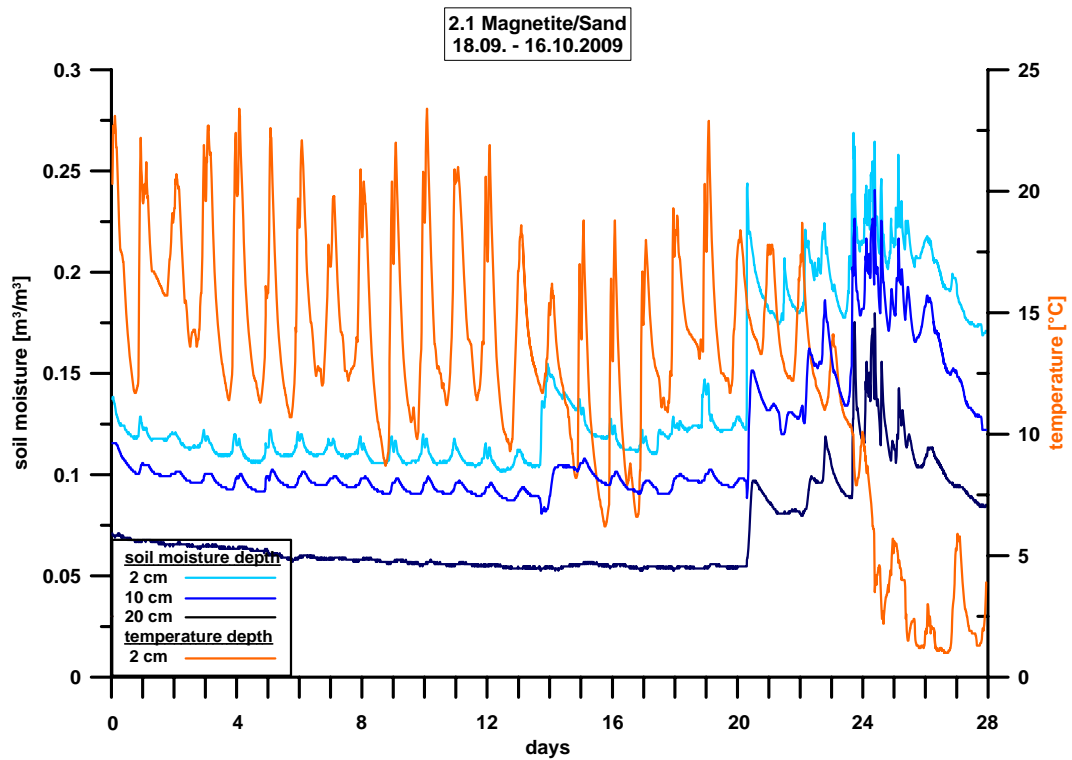


Fig. 9: Soil moisture and temperature recording in Lane 2.1 - Magnetite/sand (soil moisture is given in $\text{m}^3/\text{m}^3 = \text{soil moisture}[\%]/100$).

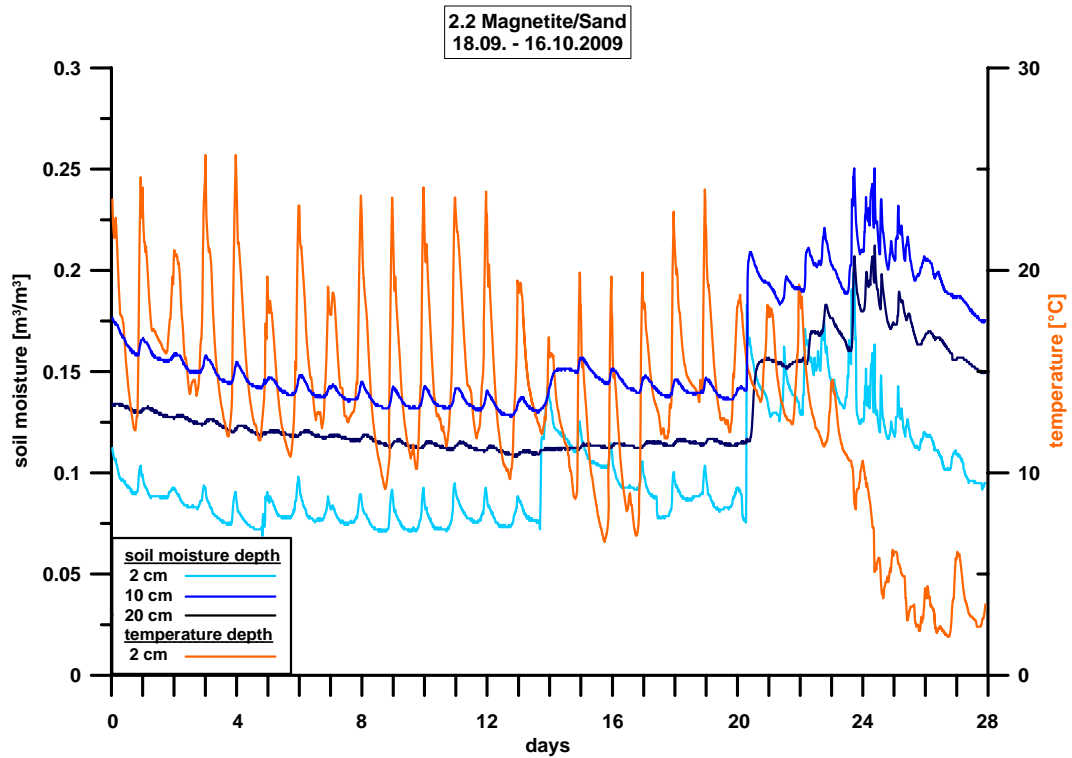


Fig. 10: Soil moisture and temperature recording in Lane 2.2 - Magnetite/sand (soil moisture is given in $m^3/m^3 = \text{soil moisture}[\%]/100$).

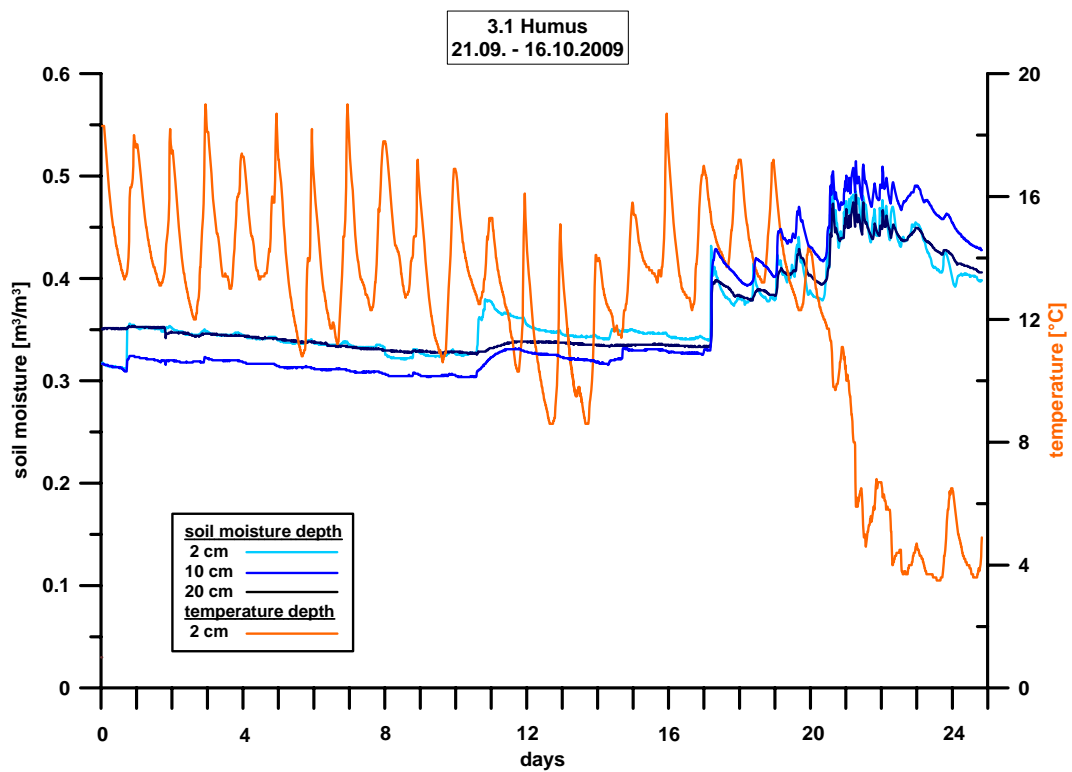


Fig. 11: Soil moisture and temperature recording in Lane 3.1 – Humus (soil moisture is given in $m^3/m^3 = \text{soil moisture}[\%]/100$).

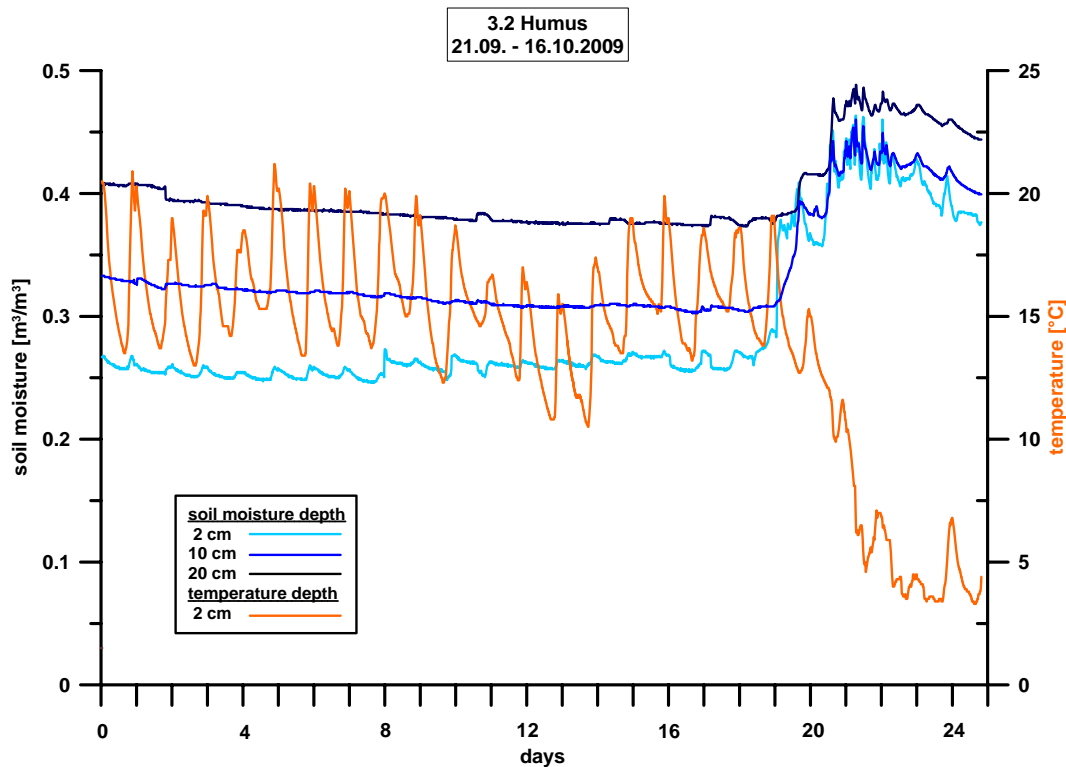


Fig. 12: Soil moisture and temperature recording in Lane 3.2 – Humus (soil moisture is given in $\text{m}^3/\text{m}^3 = \text{soil moisture}[\%]/100$).

4.1.3 Spatial variability of soil moisture and dielectric constant (relative permittivity)

Soil water content and the related dielectric constant are the main factors that are influencing the performance of GPR. It determines how the GPR antenna couples to the soil or which part of the emitted energy is reflected at the soil surface. On the other hand, a high dielectric constant of the soil yields a high contrast to the plastic or air-filled body of the mines which is expected to increase the detectability. The spatial variation of this parameter is an additional factor for the influence on the performance of GPR sensors. A high variability of the dielectric constant can deteriorate the performance and can be a cause for false alarms and missed mines at the worst. For an according characterisation of the test lanes the dielectric constant was investigated by means of a TDR probe in the training lanes. Measurements were carried out on a transect with a point distance of 10 cm. The results are displayed in Figs.13-15 and the respective statistical parameters are given in Table 5.

The figures visualise the heterogeneity of soil moisture and dielectric constant in the test lanes. Only the coarse sandy which is relatively dry substrate of the “Magnetite” lane (Lane 2.3) shows a low spatial variance. But the absolute values of the clay loam of the “Laterite” lane (Lane 1.3) and the loam of the “Humus” lane (Lane 3.3) are three to four times higher. They also show high spatial variability that is expressed in the coefficient of variation of 18 and 19%. The correlation lengths are a measure for the spatial change of the property. Since the absolute values and the heterogeneity of the “Magnetite” lane (Lane 2.1) are too low, a correlation length cannot be determined. The two other training lanes show correlation lengths of 1.35 and 0.63 m which indicates the short distances on which a change of the respective

physical property can occur. Reasons for the spatial variability of soil moisture in these test lanes are inhomogeneities of soil texture, humus content and compaction of the soil. In lane 3.3 “Humus” the high stone content has additionally a particular influence on the heterogeneity of soil water content.

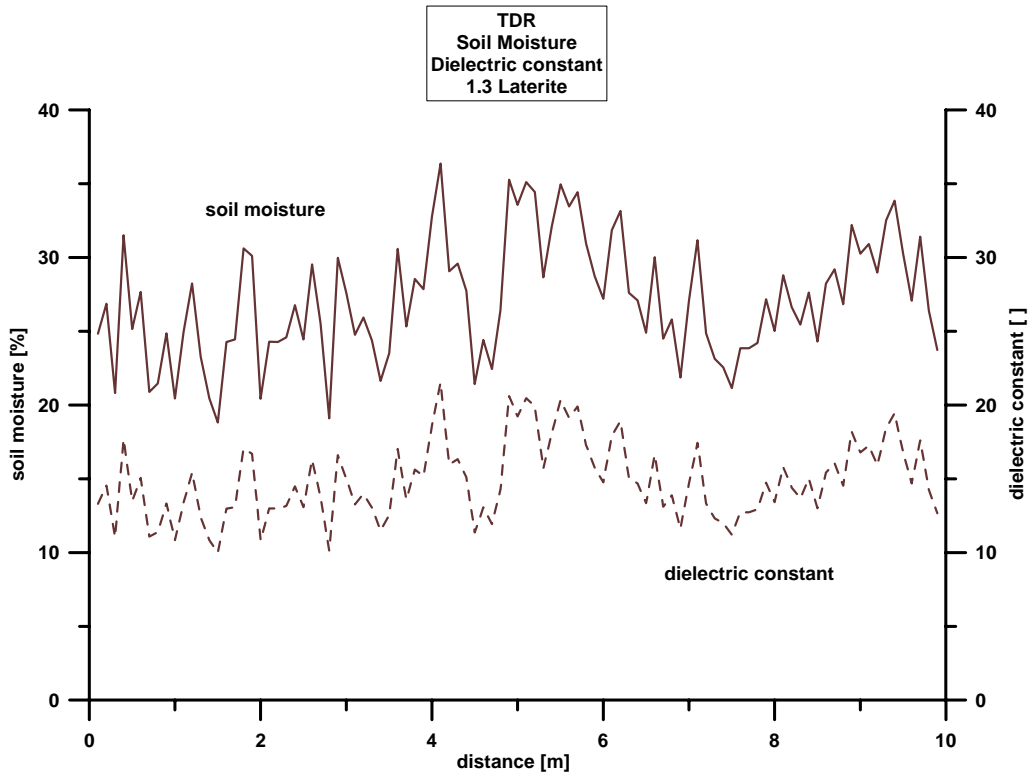


Fig. 13: Soil moisture and dielectric constant in lane 1.3 Laterite, measured on 17.09.2009.

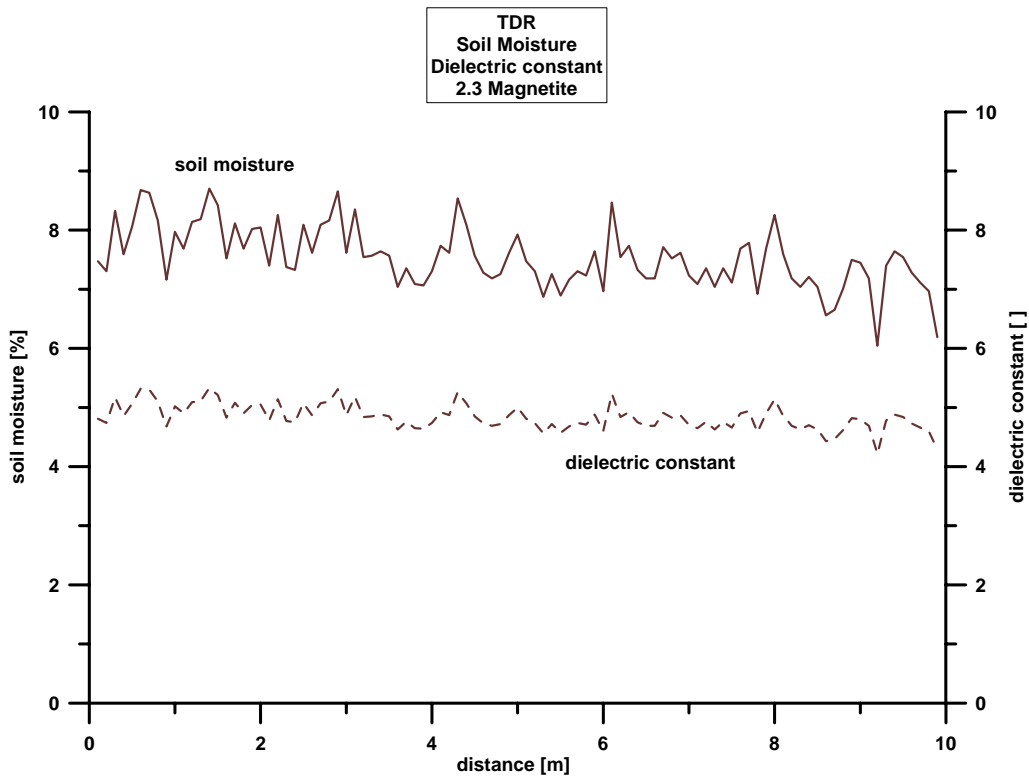


Fig. 14. Soil moisture and dielectric constant in lane 2.3 Magnetite/Sand, measured on 16.09.2009.

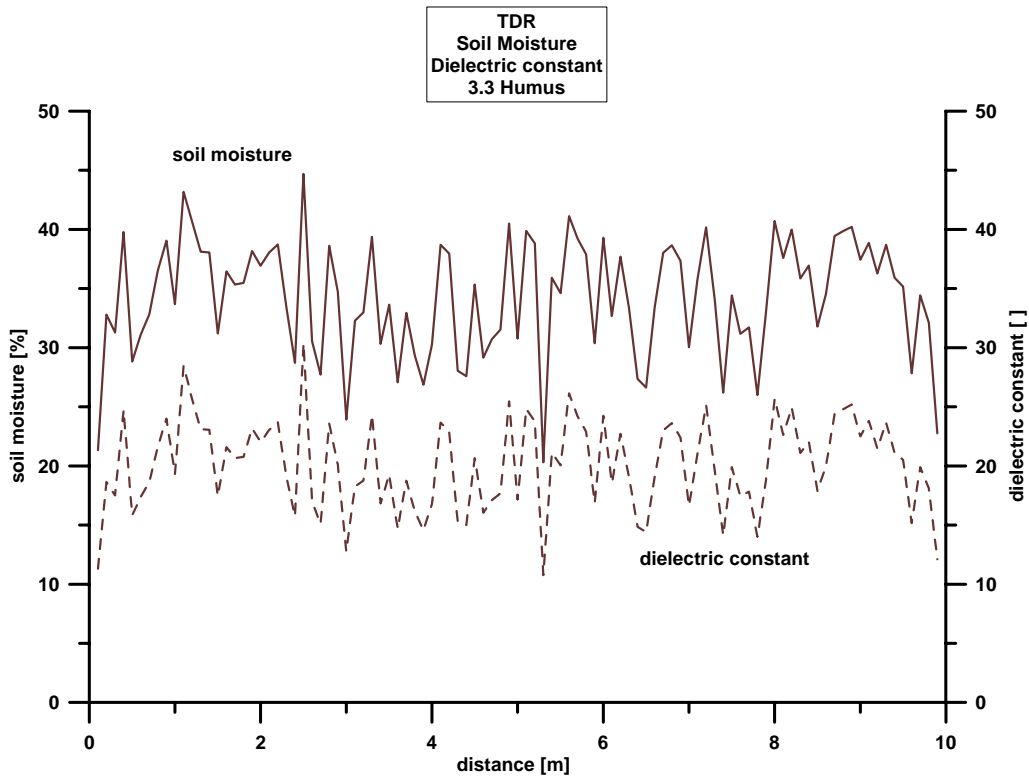


Fig. 15: Soil moisture and dielectric constant in lane 3.3 Humus, measured on 17.09.2009.

Table 5: Parameters describing the spatial variability of soil moisture.

		1.3 Laterite	2.3 Magnetite	3.3 Humus
Measured date		17.09.09	16.09.09	17.09.09
Dielectric constant []	mean	14.9	4.8	20.1
	standard deviation	± 2.7	± 0.2	± 3.9
	coefficient of variation [%]	18	4	19
Soil moisture [%]	mean	27.1	7.6	34.2
	standard deviation	± 4.1	± 0.5	± 5.0
	coefficient of variation [%]	15	7	14
Correlation length [m]		1.35	-*	0.63

* Value could not be determined

4.1.4 Ground-penetrating radar (GPR) measurements

GPR measurements with ground coupled and shielded 1.5 GHz antennas were carried out on the training lanes to observe the influence of the different soil textures on the detectability of the targets. Dielectric constant is the main factor that affects GPR performance and hence the soil water content and its spatial distribution have the biggest influence on the detectability, besides stones.

In Fig. 16 one can notice that the mines are clearly visible with their diffraction hyperbolas in the coarse sandy test lane (“Magnetite/Sand”, Lane 2.4). Due to the higher permittivity of the moist clayey loamy Laterite, antenna coupling and radiation pattern changes and the diffraction hyperbolas are smaller but can still be identified. In the stony loam of the “Humus” test lane (Lane 3.4), permittivity and radiation pattern is comparable to the Laterite. But, reflections caused by the soil heterogeneities are higher and superimpose the mine signal so that some of the mines, in particular the deeper ones, cannot be recognised any more.

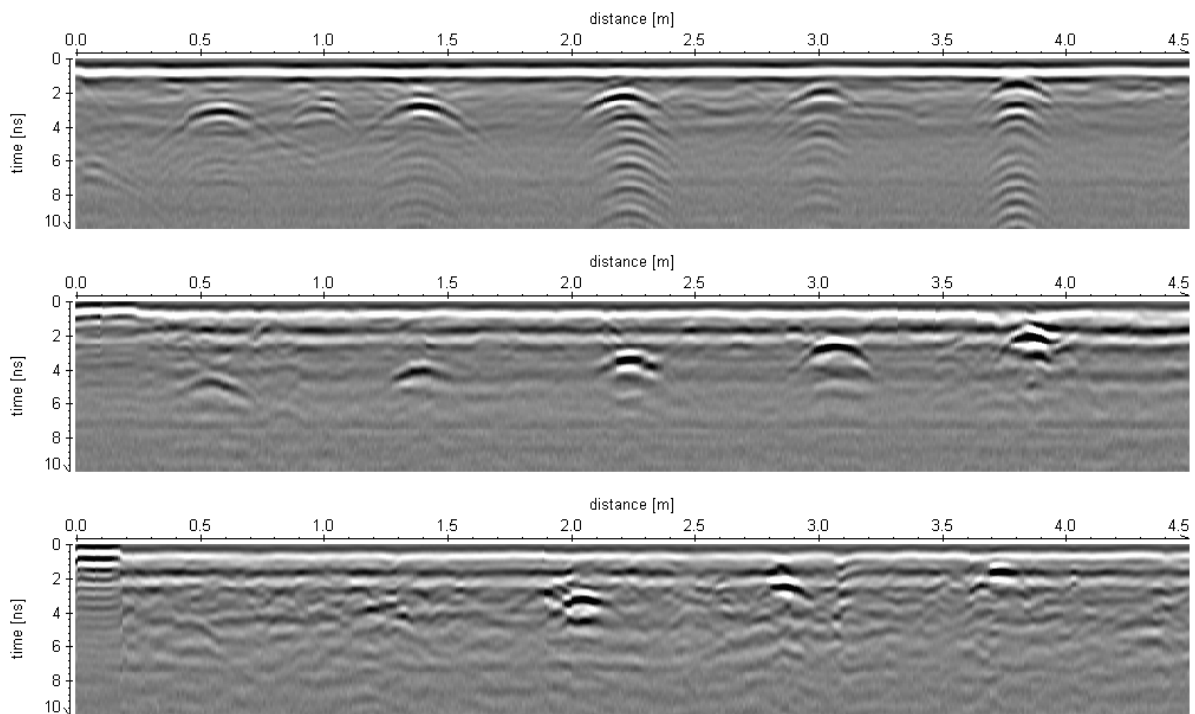


Fig. 16: GPR profiles along training lanes (1.5 GHz GSSI antenna). Top: Lane 2.4 (“Magnetite/Sand”), middle: Lane 1.4 (“Laterite”, clay loam), bottom: Lane 3.4 (“Humus”, loam, stony). PPM-2 mines were placed with a spacing of approximately 60 cm at a depths of 25, 20, 15, 10 and 5 cm (from left to right). The amplitudes are normalised to the maximum within each radargram..

4.1.5 Geoelectrical measurements

The electric conductivity of soils relies mainly on texture, salinity, moisture and humus content. Geoelectrical measurements were carried out with 3 cm long electrodes and a spacing of 10 cm. The electrodes were arranged either on several parallel 10 m long profiles or on a regular grid covering an area of 0.7 by 1.5 m. On the training lanes the longer profiles could be measured whereas on the test lanes we had to restrict to the small areas where no targets were buried. Apparent conductivity was measured in dipole-dipole configuration. All longitudinal and radial dipole configurations of the first two dipole widths were measured and the data were inverted resulting in a resistivity distribution of the upper half meter of the soil.

Measurements on test lanes

A two-dimensional area for the investigation was located in the middle of each lane, which was free of targets, and the measurements were accomplished in the days before the dual sensor test started. A measuring array is pictured in Fig. 17. The aim of this investigation was to characterise the three-dimensional variation of electric conductivity and with it the textural structure and water distribution of the test lane. The following figures show the inverted results for 7 different depths (Figs. 18-25).



Fig. 17: Geoelectrical measuring array in test lane 1.1 “Laterite”.



Fig. 18: Soil electric conductivity at depths from 5 cm to 35 cm in Lane 1.1 (Laterite), measured on 21.09.2009.

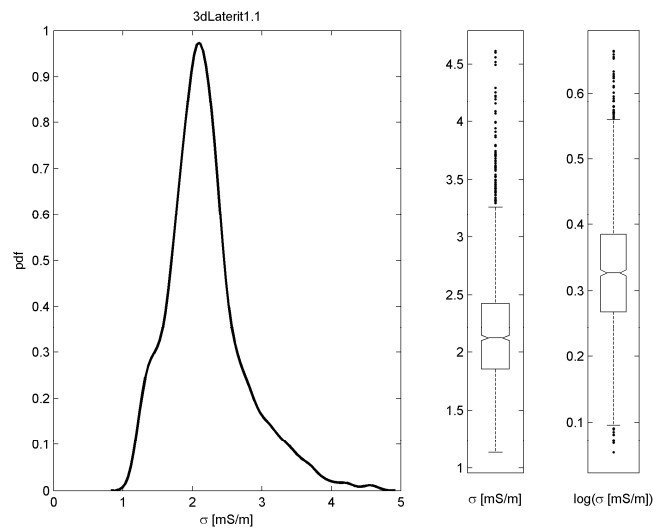


Fig. 19: Probability density function (pdf) of the electric conductivity in Lane 1.1 (Laterite), measured on 21.09.2009.

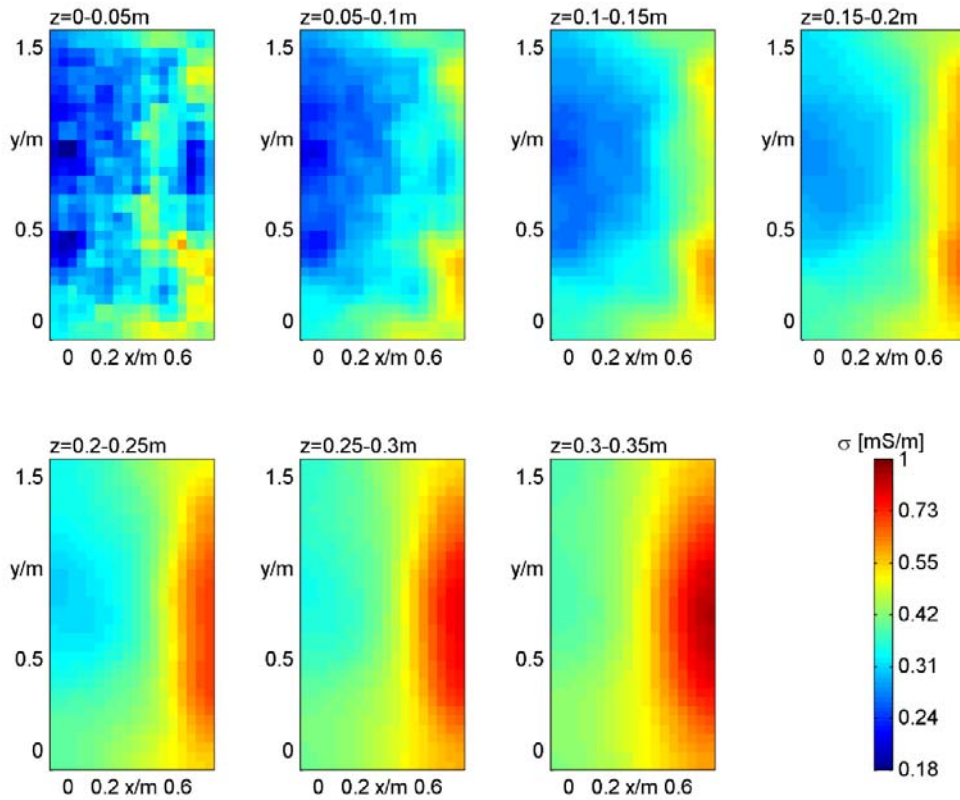


Fig. 20: Soil electric conductivity at depths from 5 cm to 35 cm in Lane 2.2. (Magnetite) , measured on 23.09.2009.

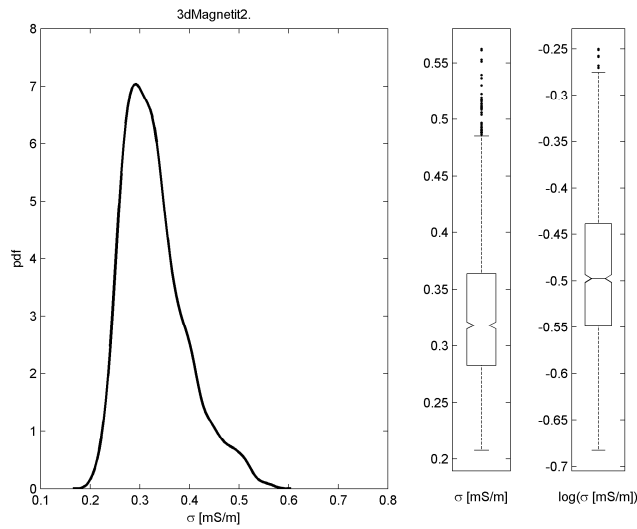


Fig. 21: Probability density function (pdf) of the electric conductivity in Lane 2.2 (Magnetite), measured on 23.09.2009

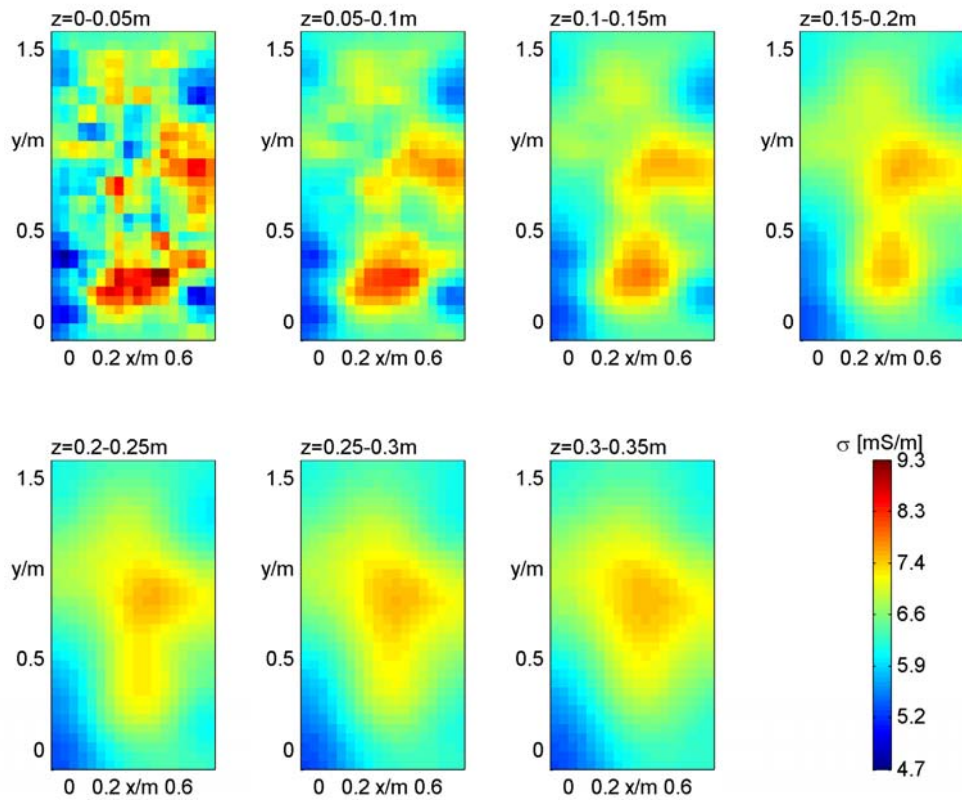


Fig. 22: Soil electric conductivity at depths from 5 cm to 35 cm in Lane 3.1 (Humus), measured on 22.09.2009.

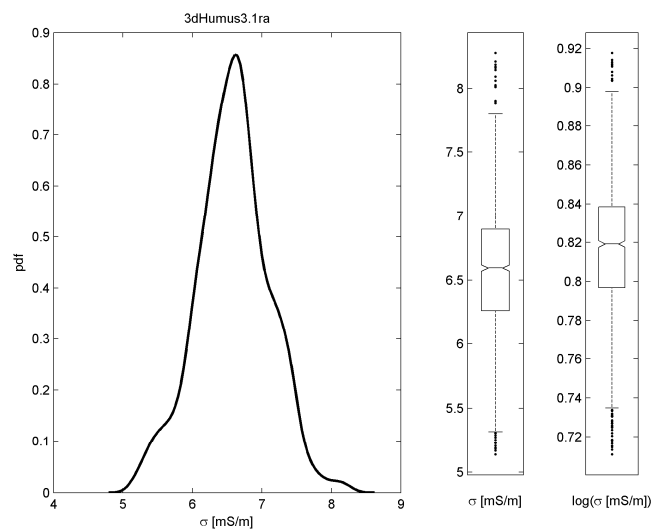


Fig. 23: Probability density function (pdf) of the electric conductivity in Lane 3.1 (Humus), measured on 22.09.2009.

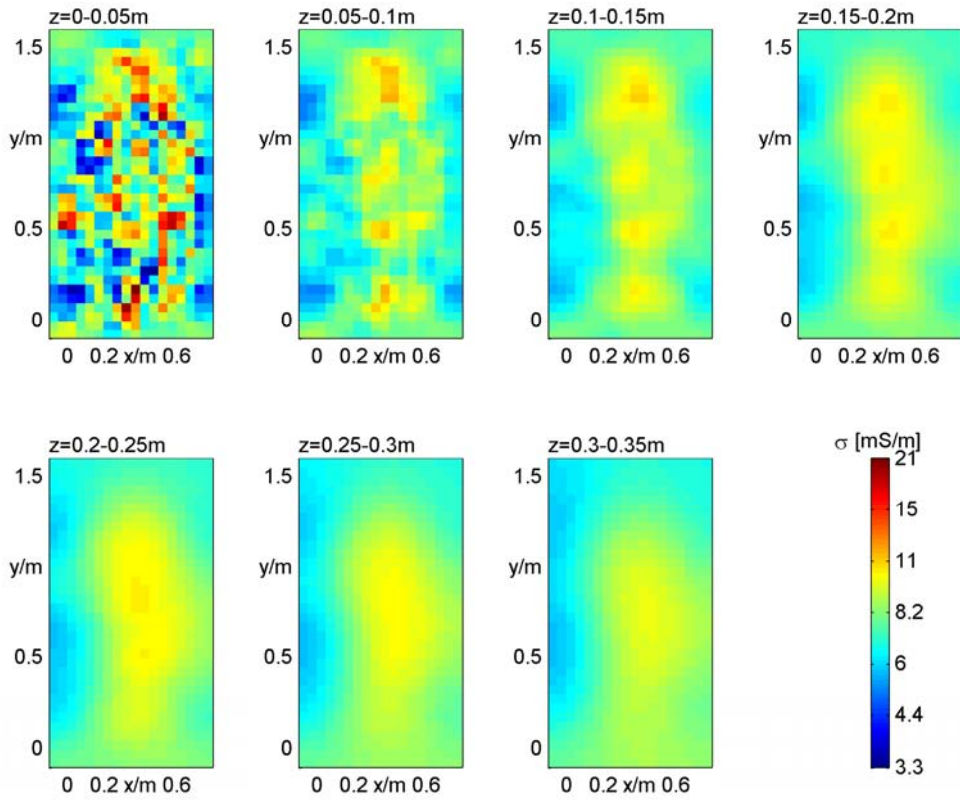


Fig. 24: Soil electric conductivity at depths from 5 cm to 35 cm in Lane 3.2 (Humus), measured on 22.09.2009.

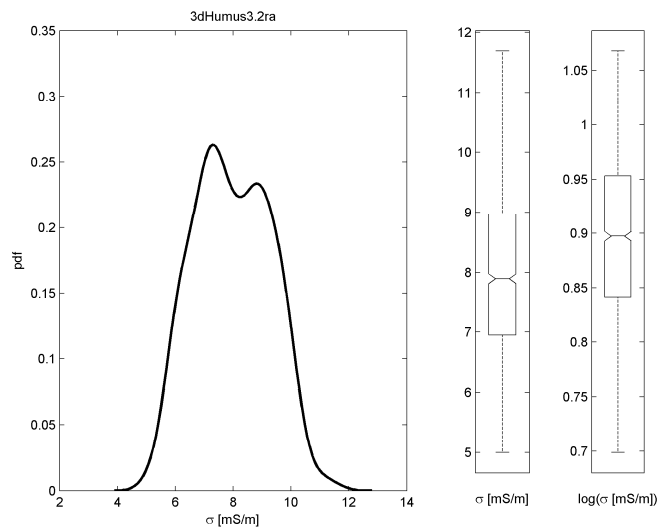


Fig. 25: Probability density function (pdf) of the electric conductivity in Lane 3.2 (Humus), measured on 22.09.2009.

Geoelectrical profiles in the training lanes

Three parallel transects in the middle of the 10 m long training lanes were measured consecutively. Fig. 26 shows the respective measuring array. The results of the inverted data and the geostatistical analysis are shown in Figs. 27-32.

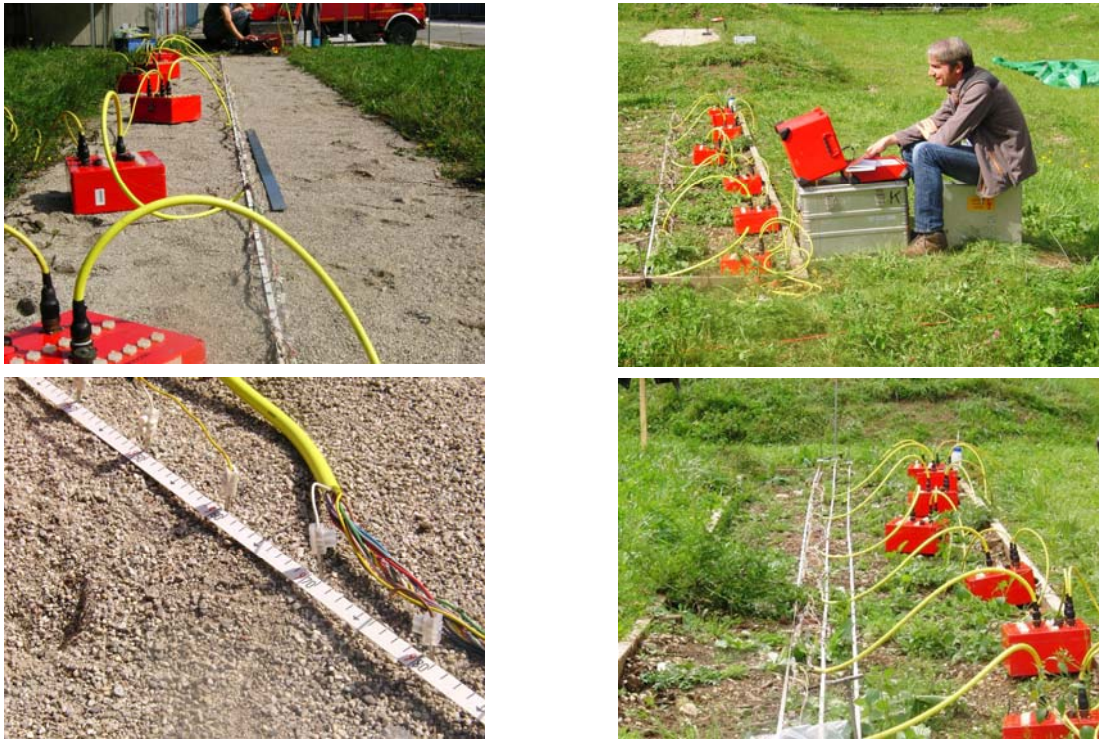


Fig. 26: Geoelectrical measuring array in training lanes 2.3 “Magnetite/Sand” (left hand) and 3.3 “Humus” (right hand).

With exception of the coarse-grained sandy magnetite for which the coupling of the electrodes was bad, data quality on the other lanes was good. As the resolution of the geoelectrical measurements decreases with depth (approx. 0.1 m resolution at the surface and 0.25 m at a depths of 50 cm), the small-scale variability is under-estimated for the subsoils.

All soils have medium to low conductivities which should not cause severe problems to neither GPR nor MD. One would assume that the Laterite possesses higher conductivity due to its high clay content and soil moisture. The discrepancy can be explained as follows: The lateritic soil is very old and was subject to strong chemical weathering in a tropical climate. This process favours the formation of 2-sheet clay minerals, mainly kaolinite, that possess only a low cation exchange capacity and thus a low electric conductivity. The Humus soils have the highest conductivities as they are much younger and were mainly subject to physical weathering and only slight chemical weathering during the current warm period. Under these conditions mainly 3-sheet clay minerals were formed that have a much higher cation exchange capacity that contributes to a higher bulk electric conductivity. Additionally the distinct electric properties of the humic substances increase the electric conductivity of these soils.

The data from the training lanes show higher variability as the data on the corresponding test lanes. This may be caused by different compaction of the soils as many people walked on the training lanes or even dug holes to bury objects or by the fact that data on the training lanes represent a 10 m long transect whereas the measurement area in the test lane is only approx. 1 m². “Humus” lane 3.3) shows high variability which is obviously caused by the high stone and root content. The sandy Magnetite shows an increase of conductivity with depth that is caused by a dry top layer but shows no lateral variability (cf. Fig. 20). The increase of conductivity with depth is not so large in the Humus soils and Laterite, due to their finer texture. The surface of the Humus and Laterite soils does not dry out as rapidly as the Sand does. The “Humus” test lane (Lane 3.2, Fig. 24) shows very high heterogeneity in the first layer which is probably caused by different electrode coupling but we can see no structures any more in deeper layers. This is due to the fact that the test lane is fairly new and there is no vegetation and thus soil moisture distribution and conductivity is homogeneous. The area of 0.6 m x 1.6 m is too small for determining correlation length by means of variogram analysis, so that they are given only for the training lanes.

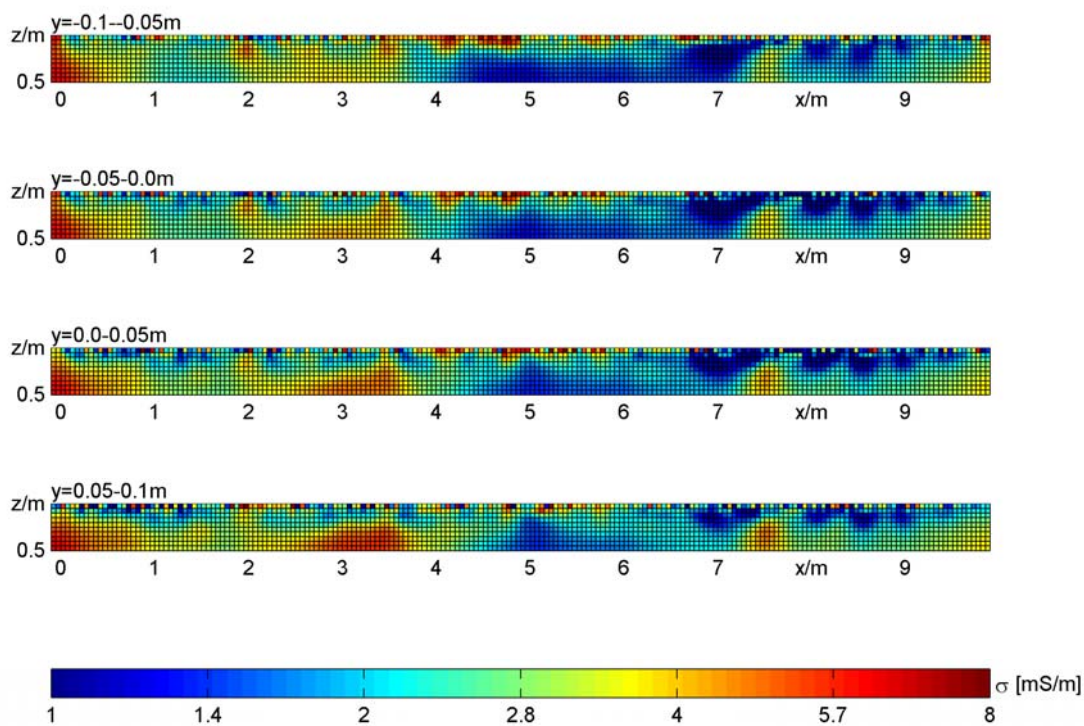


Fig. 27: Soil electric conductivity in Lane 1.3 (Laterite), measured on 17.09.2009.

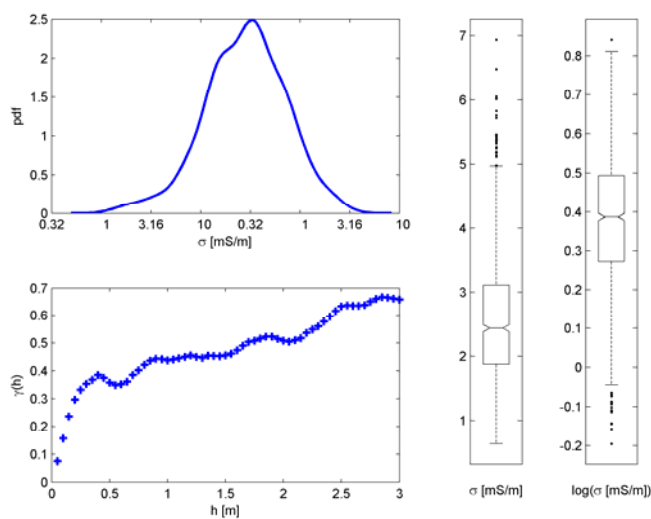


Fig. 28: Geostatistical analysis of topsoil electric conductivity ($z = 0.05$ - 0.20 m) of Fig. 27. Boxplots (right), probability density function (top), semivariogram (bottom) which determines the correlation length of 30 cm.

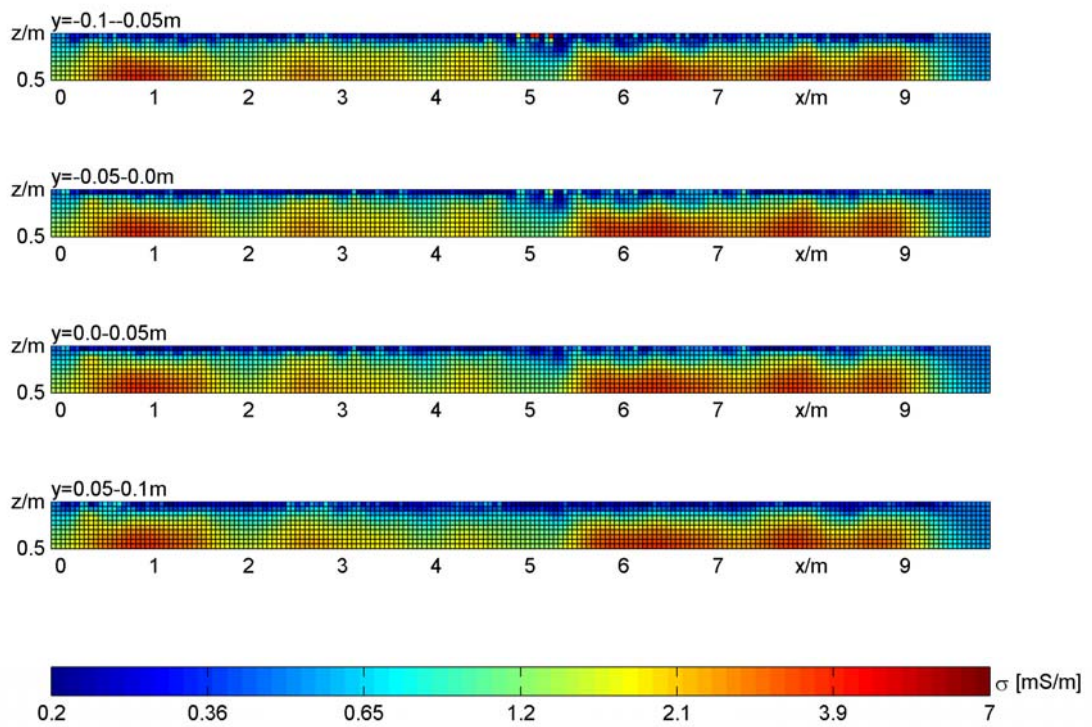


Fig. 29: Soil electric conductivity in Lane 2.3 (Magnetite), measured on 15.09.2009.

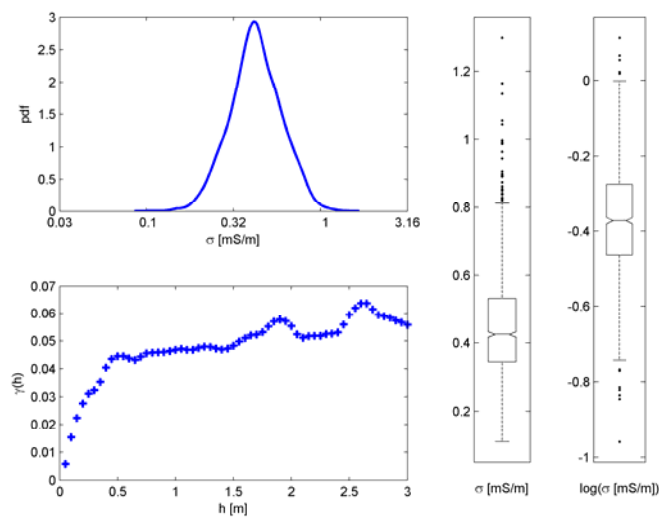


Fig. 30: Geostatistical analysis of topsoil electric conductivity ($z = 0.05-0.20$ m) of Fig. 29. Boxplots (right), probability density function (top), semivariogram (bottom) which determines the correlation length of 50 cm.

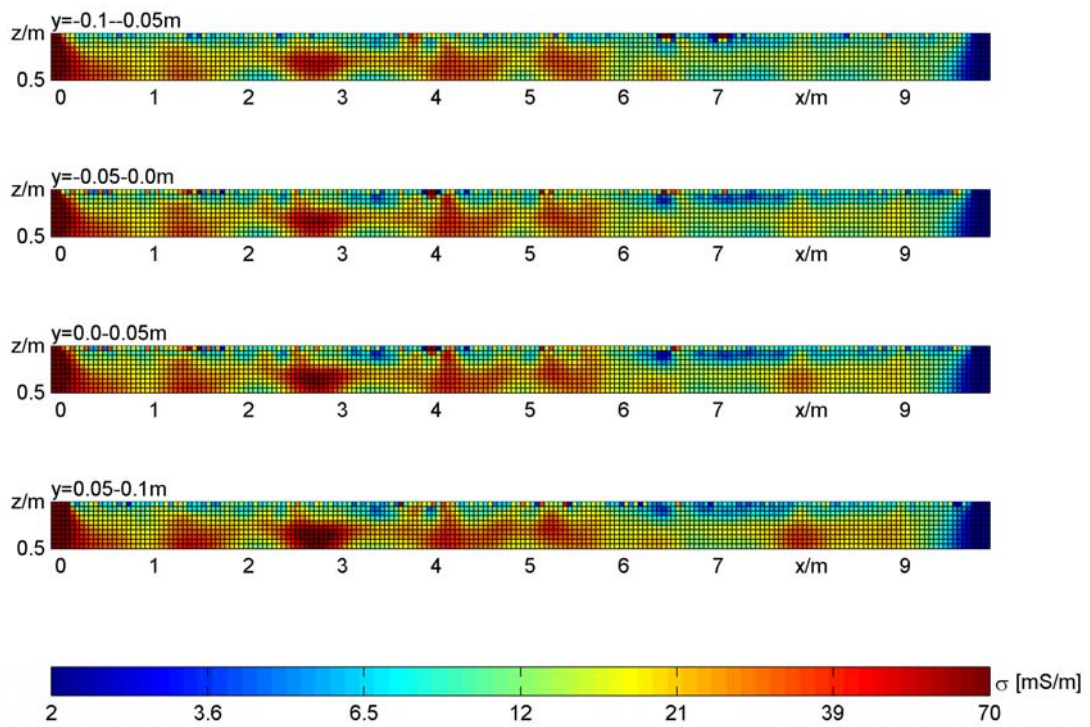


Fig. 31: Soil electric conductivity in Lane 3.3 (Humus), measured on 16.09.2009.

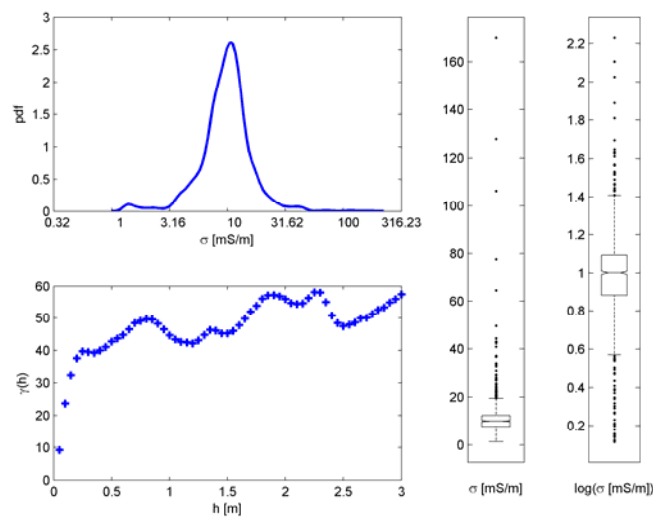


Fig. 32: Geostatistical analysis of topsoil electric conductivity ($z = 0.05-0.20$ m) of Fig. 31. Boxplots (right), probability density function (top), semivariogram (bottom) which determines the correlation length of 25 cm.

A comparative appraisal of the electric conductivities can be done by means of Table 6.

As with the exception of Humus lane 3.1 the test soils were not covered with comprehensive vegetation and the lanes were build only a few months prior to the test. Thus, spatial distribution of electric conductivity does not correspond to typical patterns that can be found in the field but show some more non-correlated random pattern.

Table 6: Summary of soil electric parameters of the test lanes. The standard deviation is also given as a measure of variability in %, although conductivity distribution is similar to a log-normal distribution. One has to notice that standard deviation does not describe the 68% population in this case.

Test Lane	mean	median	standard deviation	coefficient of variation	correlation length
	[mS/m]		[mS/m]	[%]	[cm]
1.1 Laterite	2.2	2.1	0.6	27.2	-
1.3 Laterite	2.6	2.4	1.0	38.5	30
2.2 Magnetite	0.33	0.32	0.06	18.2	-
2.3 Magnetite	0.45	0.42	0.15	33.3	50
3.1 Humus	6.6	6.6	0.52	7.9	-
3.2 Humus	8.0	7.9	1.3	16.3	-
3.3 Humus	11.1	10.0	8.8	79.2	25

4.2 Laboratory measurements

4.2.1 Frequency dependence of electric conductivity

The frequency dependence of electric conductivity was determined by laboratory measurements because it is considered as being a factor that can influence the performance of metal detectors. Although its impact on detection technique is still under discussion and there are no means to evaluate the measuring results. The investigation was carried out to find out whether the test soils show differences with respect to this property. The measurements were carried out on water-saturated samples.

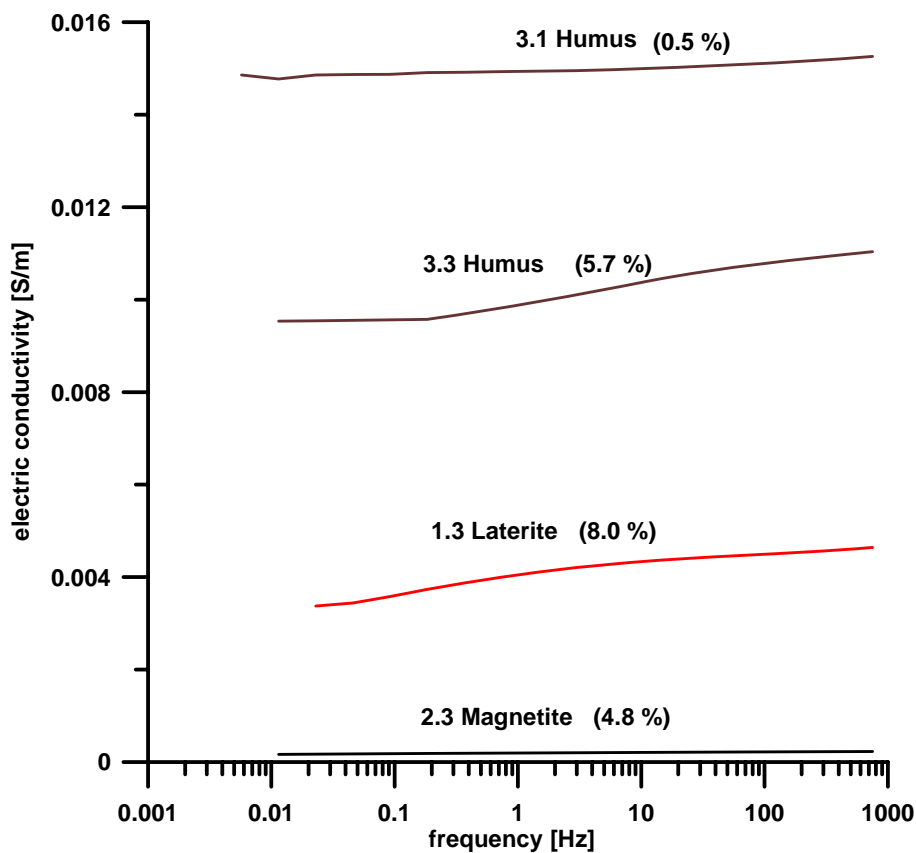


Fig. 33: Laboratory measurements of soil electric conductivity by spectral induced polarization (SIP). The frequency dependence over one decade is given in parentheses.

The mean values of the measured electric conductivities are very different; this is due to the proportion of electric conducting humous and clayey particles. The frequency dependencies show clear differences as well. Soils with higher frequency dependence have either a higher humus content (Lane 3.3) or clay content (Lane 1.3) than the others. The frequency dependence of the coarse sand of the “Magnetite/Sand” lane (Lane 2.3) cannot be deduced and is possibly the result of too low conductivity and the associated uncertainty.

4.2.2 Frequency dependent dielectric constant (relative permittivity) of test targets

The absolute values as well as the frequency dependence of permittivities of the test targets are of importance as to the performance of the GPR. It further refers to the question whether the test targets comprise realistic dielectric features compared to real landmines.

The real parts of the dielectric constant of the plastic body of the ERA calibration target and its wax filling as well as the PPM-2 and the silicone filling show the normal behaviour of solid matter consisting of single-component non polarisable materials (Figs. 34 and 35). Their dielectric constants are around 3 and they show no frequency dependencies. The imaginary parts are very low and are below the measuring accuracy of the device. Therefore they are not shown here.

Slightly different is the result of the Gyata-64 (PMN) plastic body which shows a dielectric constant of 6 and an observable frequency dependence. The imaginary part is increased and measurable compared to the other plastic casings (Fig. 36).

The most remarkable measuring result is from the elastic rubber cap of the Gyata-64 (PMN) target. This material shows both a high real part and a high imaginary part and a high frequency dependence as well (Fig. 37).

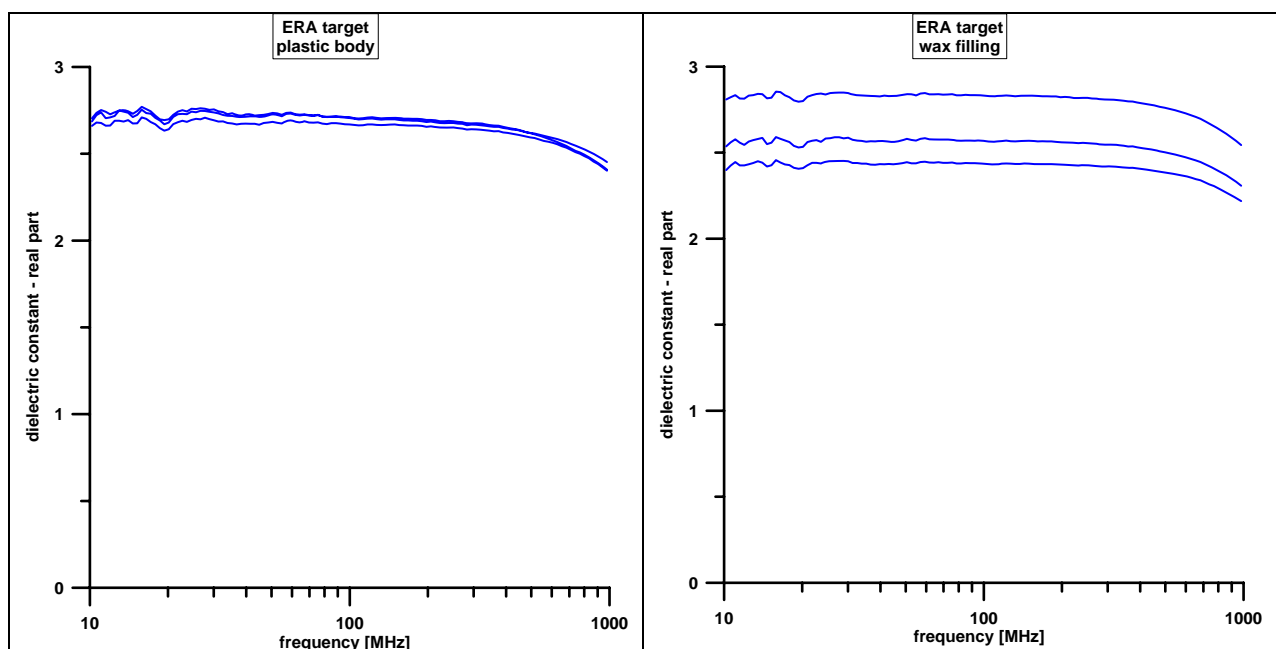


Fig. 34: Real part of the frequency dependent dielectric constant of the ERA calibration target casing (left) and the wax filling (right).

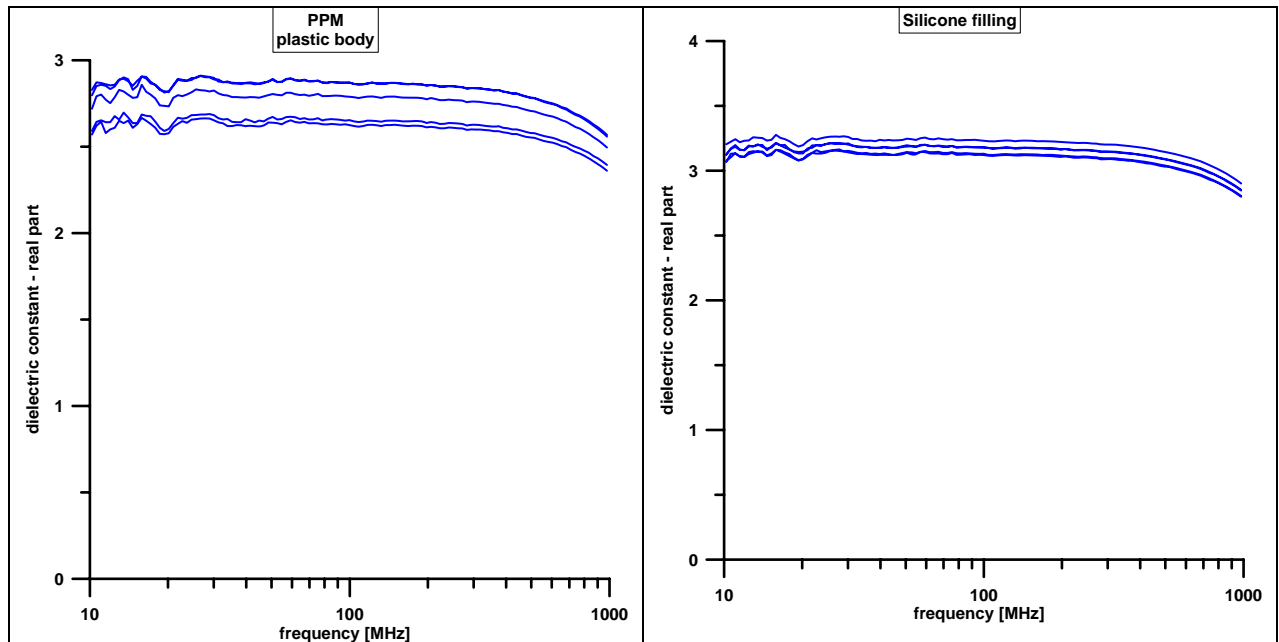


Fig. 35: Real part of the frequency dependent dielectric constant of the PPM-2 plastic body(left) and the silicone filling “3110 Base + Catalyst 1” (right).

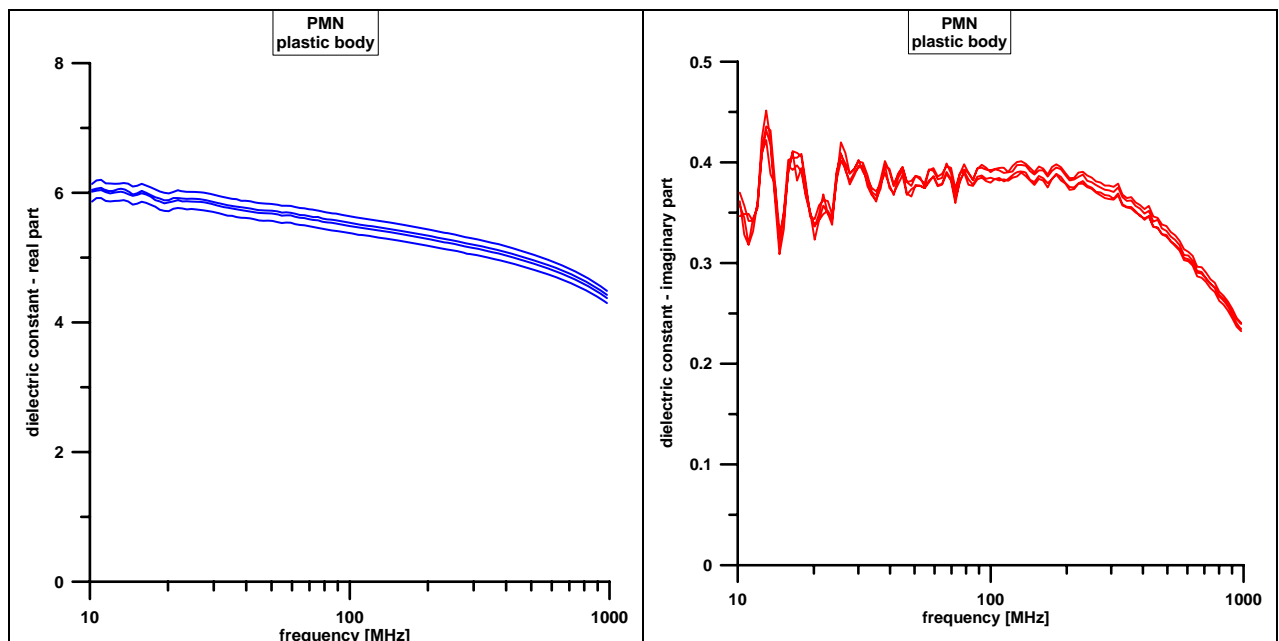


Fig. 36: Real part (left) and imaginary part (right) of the frequency dependent dielectric constant of the Gyata-64 (PMN) plastic casing.

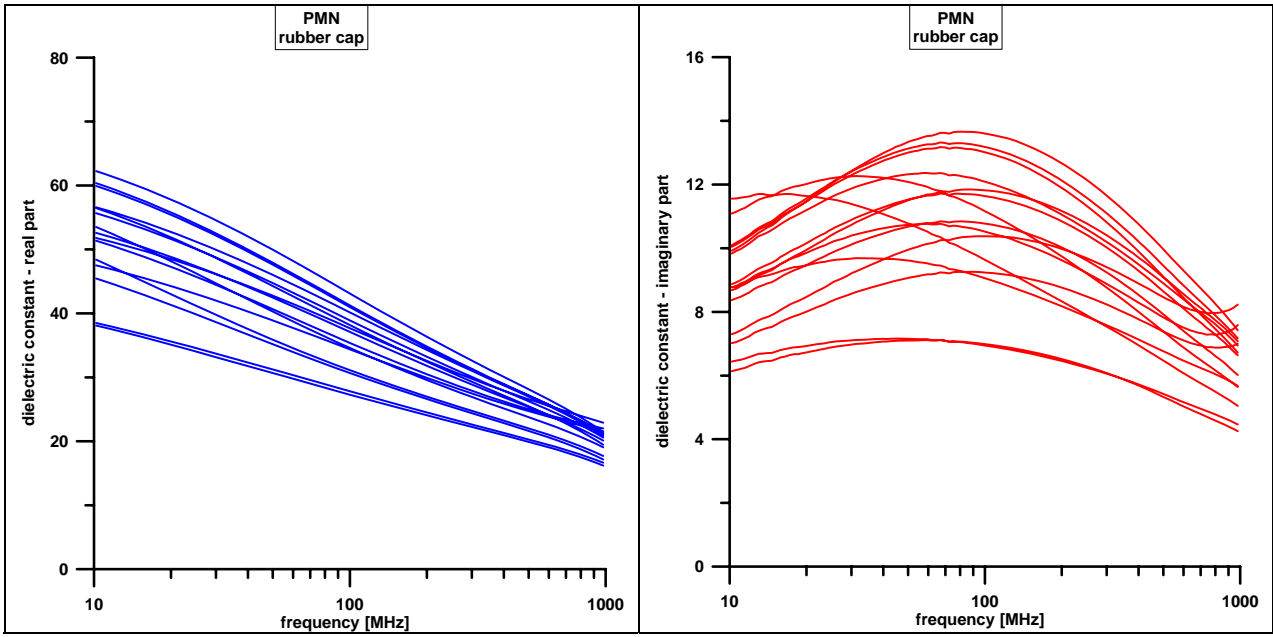


Fig. 37: Real part (left) and imaginary part (right) of the frequency dependent dielectric constant of the Gyata-64 (PMN) rubber cap.

5 Soil magnetic properties

5.1 Field measurements

Soil magnetic susceptibility and its frequency dependence are the main factors that have an influence on the performance of metal detectors. Whilst most modern detector types have a good capability to compensate the influence of absolute magnetic susceptibility, the frequency dependence remains a deteriorating factor for many of the instruments. However, the investigation of absolute magnetic susceptibility is still of importance because high absolute values are still the precondition for the occurrence of high absolute frequency dependencies that might hamper detector performance. A further factor that can have a negative effect on metal detectors is the heterogeneity of magnetic susceptibility which can constrain the ground compensation of various detectors and can cause false alarms in places. Therefore, and because only absolute magnetic susceptibility can be measured in the field, its spatial variation in the training lanes was investigated with a field loop. It was not possible to carry out this investigation in the test-lanes because of the buried targets that would adulterate the measurement readings of the soils. The measurements were carried out in the same way as the TDR measurements, on a transect with a measuring distance of 10 cm. The results are displayed in Figs. 38-40 and the respective statistical parameters are given in Table 7.

With reference to the thresholds in Table 9 the soils in the “Laterite” (Lane 1.3) and the “Magnetite/Sand” lane (Lane 2.3) can be classified as providing a very severe influence on single frequency continuous wave metal detectors. On the other hand, the substrate of the “Humus” lane (Lane 3.3) is apparently neutral. However, the graphs reveal different spatial heterogeneities that are quantified by the statistical data in Table 7. The heterogeneity in the “Humus” lane (Lane 3.3) is extreme but it is questionable if that affects metal detector performance because all the values remain in the neutral range. Such an influence is more expectable in the “Laterite” (Lane 1.3) lane where susceptibility is high and spatial variability is noticeable.

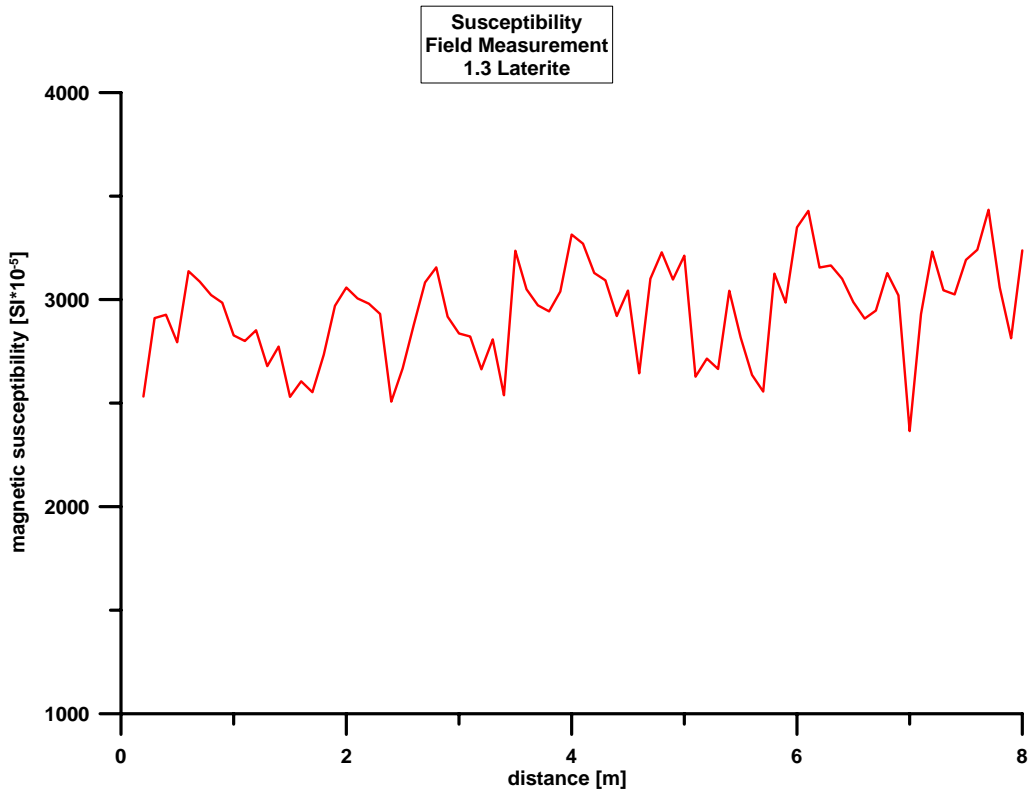


Fig. 38: Soil magnetic susceptibility in Lane 1.3 (Laterite), measured with field loop.

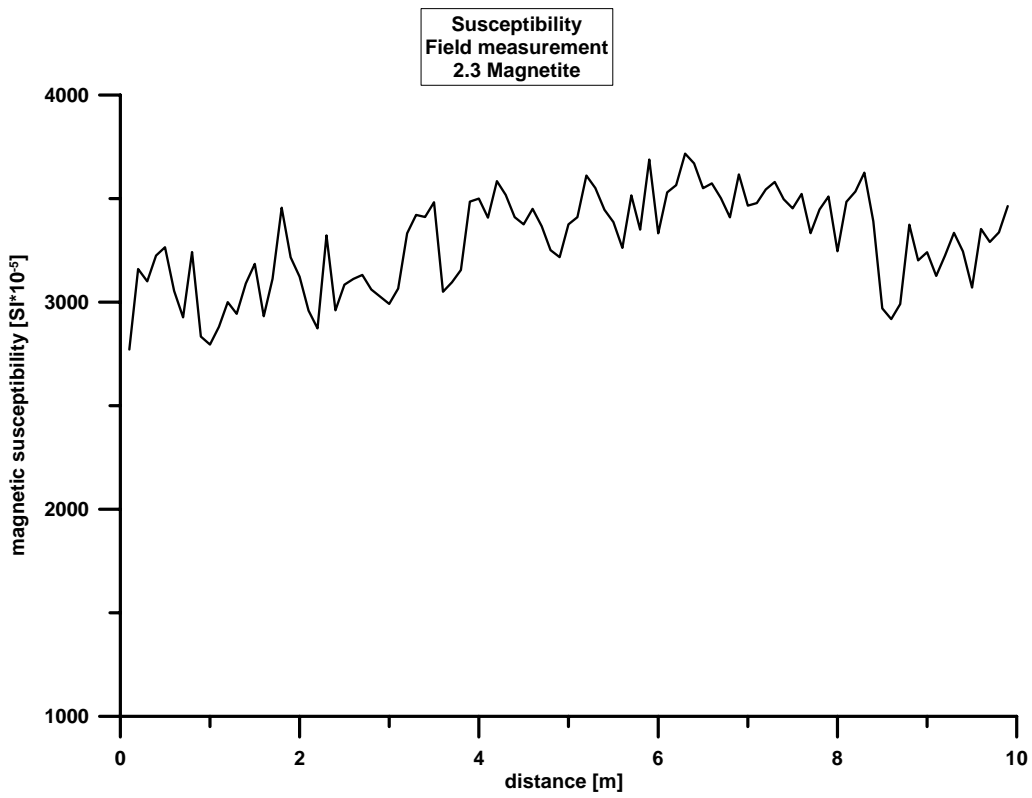


Fig. 39: Soil magnetic susceptibility in Lane 2.3 (Magnetite), measured with field loop.

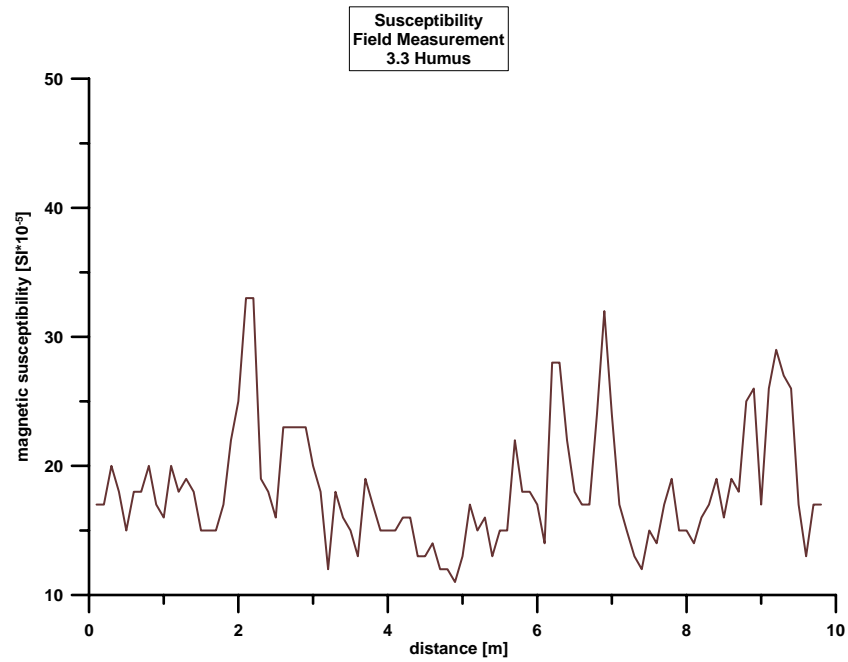


Fig. 40: Soil magnetic susceptibility in Lane 3.3 (Humus), measured with field loop.

Table 7: Summary of soil magnetic field parameters of the test lanes.

Magnetic susceptibility		1.3 Laterite	2.3 Magnetite	3.3 Humus
mean	[SI x 10 ⁻⁵]	2977	3324	18.5
median		2986	3333	17.0
standard deviation		251	247	7.2
coefficient of variation	[%]	8.4	7.4	38.9

5.2 Laboratory measurements

5.2.1 Frequency dependence of magnetic susceptibility

The frequency dependence of magnetic susceptibility has the biggest influence on modern metal detectors because it is still problematic to compensate this effect. Samples from the test lanes were investigated in a frequency range up to 10 kHz. The results are shown in Figs. 41-44 and in Table 8.

The magnetic susceptibilities at low frequency in the laboratory measurements are much higher than those of the field measurements (see Table 7). In general this difference is higher when the spatial variability in the field is higher. The cause for much lower values in the field is because the field loop investigates a bigger volume in natural bulk density including a large volume of air and water filled pores. Additionally surface cracks and the roughness of the ground surface increase the air volume that is included in the measuring field. In laboratory measurements, on the other hand, small sized samples are used that are close-packed and thus have a higher bulk density than the natural layered topsoil horizon.

With respect to the thresholds in Table 10 the absolute values of frequency dependent magnetic susceptibility in Table 8 can be classified as follows:

- Lane 1.3 (Laterite) – very severe
- Lane 2.3 (Magnetite) – moderate
- Lane 3.1 (Humus) – moderate
- Lane 3.3 (Humus) – neutral

It is only the substrate of the “Laterite” test lane that may seriously impede the performance of modern metal detectors.

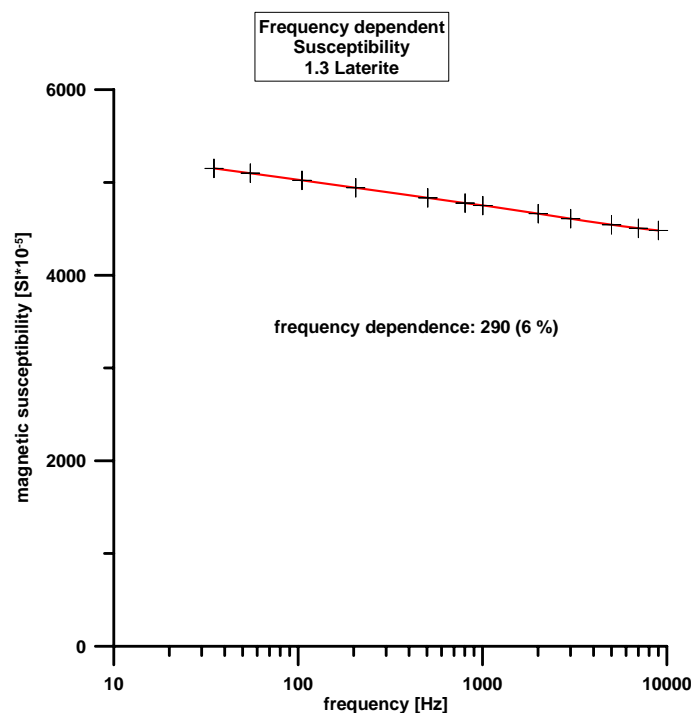


Fig. 41: Frequency dependent magnetic susceptibility in Lane 1.3 (Laterite). The frequency dependence is given for one decade (100 Hz vs. 1000 Hz).

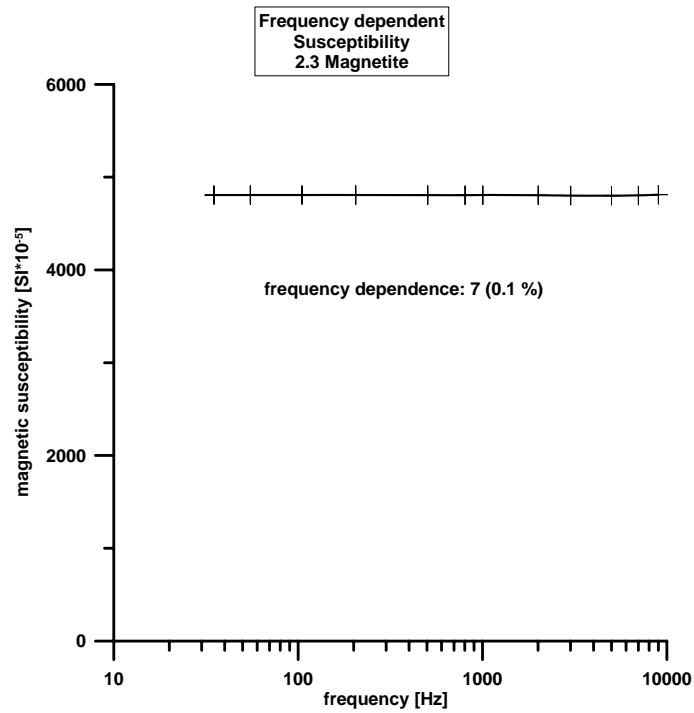


Fig. 42: Frequency dependent magnetic susceptibility in Lane 2.3 (Magnetite). The frequency dependence is given for one decade (100 Hz vs. 1000 Hz).

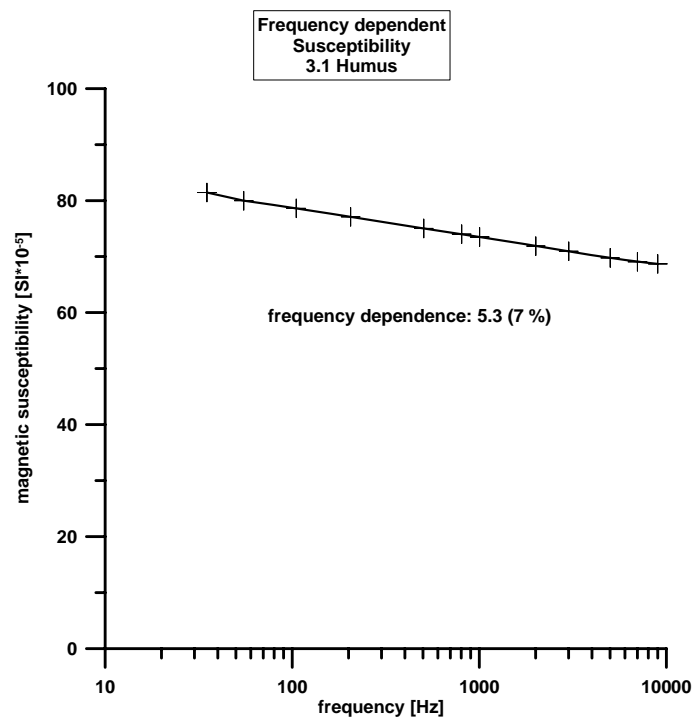


Fig. 43: Frequency dependent magnetic susceptibility in Lane 3.1 (Humus). The frequency dependence is given for one decade (100 Hz vs. 1000 Hz).

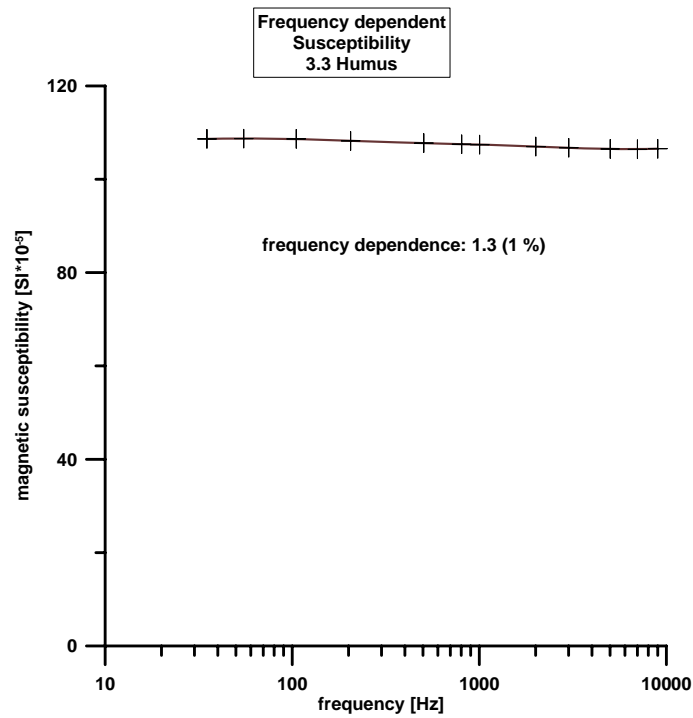


Fig. 44: Frequency dependent magnetic susceptibility in Lane 3.3 (Humus).

Table 8: Summary of soil magnetic laboratory parameters of the test lanes.

Magnetic susceptibility		1.3 Laterite	2.3 Magnetite	3.1 Humus	3.3 Humus
Low frequency*		4835	4807	75.0	108
absolute frequency dependence	[SI x 10 ⁻⁵]	290	7	5.3	1.3
relative frequency dependence	[%]	6.0	0.1	7.1	1.2

* measured at $f = 505$ Hz and a magnetic field strength of $H = 400$ A/m.

6 Comprehensive classification of the test lanes

The soil magnetic properties of the test lanes can comprehensively be classified with respect to Tables 9 and 10. The estimated overall influence is given in Table 11.

Table 9: Indicative values of magnetic susceptibility that can be expected for soil effects for single frequency continuous wave metal detectors (CEN 2008)¹.

Soil influence	Low frequency susceptibility κ [10^{-5} SI]
Neutral	< 50
Moderate	50 – 500
Severe	500 – 2000
Very severe	> 2000

Table 10: Indicative values classifying the influence of frequency dependent susceptibility on multi-frequency continuous wave and pulse induction detectors (CEN, 2008)¹.

Soil influence	Frequency dependence $\Delta\kappa$ [10^{-5} SI]
Neutral	< 5
Moderate	5 – 15
Severe	15 – 25
Very severe	> 25

To estimate soil influence on GPR performance no thresholds for soil electric properties are available, unlike magnetic susceptibility for metal detectors. Alternatively, an evaluation is made based on the results of our GPR measurements in connection with the geophysical investigation of the test lanes. The evaluation is also included in Table 11.

Table 11: Estimated impact of soil on the performance of detection techniques.

Detector	Laterite 1.1 & 1.2	Magnetite 2.1 & 2.2	Humus 3.1	Humus 3.2
Metal detector	XXX	X	O - X	O
GPR	X - XX	O	X	XXX

O neutral
 X moderate
 XX severe
 XXX very severe

¹ CEN (European Committee for Standardization). 2008. Humanitarian Mine Action - Test and Evaluation - Part 2: Soil characterization for metal detector and ground penetrating radar performance. Workshop Agreement (CWA) 14747-2. Available at http://www.itep.ws/pdf/CWA_soil_characterization.pdf. European Committee for Standardization.

Explanations for the classification in Table 11 are as follows.

“Laterite” lanes (Lanes 1.1, 1.2, 1.3 and 1.4)

The classification concerning metal detectors is very severe because of the high magnetic susceptibility and the very high frequency dependence. The remarkable spatial variability of magnetic properties can make it even more difficult.

There is probably a moderate to severe influence on GPR because of a high spatial variability of soil moisture and the dielectric constant (cf. Fig. 13) which is due to variations in bulk density. Additionally, the stone content (< 5 %) may cause some false alarms. On the other hand, the contrast between the dielectric constant of the soil (Table 5) and the one of the plastic body of the targets (Figs. 34 - 36) implies a good detectability (cf. Fig. 16). Overall the moderate electric and dielectric properties do not give reason to expect a very severe impediment of GPR.

“Magnetite/Sand” lanes (Lanes 2.1, 2.2, 2.3 and 2.4)

The overall influence on metal detectors is only moderate because of no frequency dependence despite absolute magnetic susceptibility is very high. Only some single frequency continuous wave metal detectors can thereof be hampered in a very severe manner.

With regard to GPR performance the electric properties are benign and more or less spatially homogeneous and a test demonstrates the good detectability of targets with GPR (Fig. 16, at the top).

“Humus” lane (Lane 3.1)

Due to the low magnetic susceptibility and the homogeneity of the loess substrate no influence on metal detectors is expected. Only a moderate influence on few detector types can arise because of the considerable relative frequency dependence.

The moderate electric properties of this substrate and their low variability (Table 6) do not give reason to expect a severe influence on GPR performance. But due to the dense grass vegetation on this test lane and an irregular drying of this soil a heterogeneous soil moisture pattern can be expected during the vegetation period. In the worst case this moisture pattern can cause false alarms for GPR and therefore this test lane is classified as moderate.

“Humus” lanes (Lanes 3.2, 3.3 and 3.4)

The absolute magnetic susceptibility of this material can be classified according to Table 9 as moderate but the values are in a very low range and should not cause a problem for the most of modern metal detectors. Because of very low frequency dependence the overall influence on metal detectors is therefore probably neutral.

This test lane exhibits a high content of coarse stones in connection with a high spatial variability of dielectric properties (Table 5). The variability is caused by the stone content as well as by inhomogeneities of texture, humus content and bulk density. These are the reasons for a serious impediment of detectability of targets (see Fig. 16 at the bottom) and therefore the lane is classified as providing very severe influence on GPR.

As a closing note with respect to further use of the test lanes it can be stated that the magnetic properties of the test lanes, which are related to their mineral compound will remain the same in a stable condition in future. On the other hand, the electric and dielectric properties are related to soil moisture content and, thus, will be subject to a seasonal change. That means that further metal detector tests will face the same conditions whilst the use of GPR will have to expect a possible change of soil properties.

List of symbols:

ϵ_r : dielectric constant, relative permittivity []

σ : electric conductivity [S/m]

κ : magnetic susceptibility []

μ_r : relative magnetic permeability, $\mu_r = 1 + \kappa$